

## BlastBerries: How Supernovae Affect Lyman Continuum Escape Fractions and Ionizing Photon Production in Local Analogs of High-Redshift Galaxies

MIRANDA Y. KONG,<sup>1</sup> DAVID O. JONES,<sup>2</sup> NICOLE E. DRAKOS,<sup>3</sup> SANGEETA MALHOTRA,<sup>4</sup> KARTHEIK IYER,<sup>5</sup> BRIAN C. LEMAUX,<sup>6,7</sup> ROHAN P. NAIDU,<sup>8</sup> THOMAS DE BOER,<sup>1</sup> KEN C. CHAMBERS,<sup>1</sup> JOHN FAIRLAMB,<sup>1</sup> WILLEM B. HOOGENDAM,<sup>1,\*</sup> MARK E. HUBER,<sup>1</sup> CHIEN-CHENG LIN,<sup>1</sup> THOMAS BERNARD LOWE,<sup>1</sup> EUGENE A. MAGNIER,<sup>1</sup> PALOMA MÍNGUEZ,<sup>1</sup> GREGORY S. H. PAEK,<sup>1</sup> ANGIE SCHULTZ,<sup>1</sup> AND RICHARD J. WAINSCOAT<sup>1</sup>

<sup>1</sup> Institute for Astronomy, University of Hawai‘i, 2680 Woodlawn Drive, Honolulu, HI 96822, USA

<sup>2</sup> Institute for Astronomy, University of Hawai‘i, 640 N A‘ohoku Pl, Hilo, HI 96720, USA

<sup>3</sup> University of Hawai‘i at Hilo, 200 W Kawili St, Hilo, HI 96720, USA

<sup>4</sup> Astrophysics Division, NASA Goddard Space Flight Center, Greenbelt, MD 20771, USA

<sup>5</sup> Flatiron Institute, 162 5th Avenue, New York, NY 10010, USA

<sup>6</sup> Gemini Observatory, NSF NOIRLab, 670 N. A‘ohoku Place, Hilo, Hawai‘i, 96720, USA

<sup>7</sup> Department of Physics and Astronomy, University of California, Davis, One Shields Ave., Davis, CA 95616, USA

<sup>8</sup> MIT Kavli Institute for Astrophysics and Space Research, 77 Massachusetts Avenue, Cambridge, MA 02139, USA

### ABSTRACT

While compact, star-forming galaxies are believed to play a key role in cosmic reionization, the physical mechanisms enabling the escape of ionizing photons through the galactic interstellar medium remain unclear. Supernova (SN) feedback is one possible mechanism for clearing neutral gas channels to allow the escape of Lyman continuum photons. Here, we use SN discoveries in low-redshift analogs of high-redshift star-forming galaxies — Green Pea galaxies and their even lower-redshift counterparts, Blueberry (BB) galaxies — to understand how SNe shape the properties of their host galaxies at high redshifts. We cross-match 1242 BB galaxies with transient discovery reports and identify 11 SNe, ten of which are likely core-collapse SNe, and compare their hosts to the larger BB population. We find that SN-hosting BBs exhibit elevated star formation rates, burstier star formation histories within the last  $\sim 50$  Myr, and higher stellar masses. We estimate the occurrence rates of SNe in BB galaxies, finding that the SN rate may be slightly suppressed in BBs compared to field galaxies of similar mass, but we are unable to fully control for observational uncertainties. Finally, SN hosts show bluer UV slopes than non-host BB galaxies at  $2.1\sigma$  significance and lower ionizing photon production efficiency at  $7.9\sigma$  significance; the former result offers modest support for the hypothesis that SN-driven feedback plays a role in facilitating the escape of ionizing photons, while the latter may imply that SN-driven quenching decreases the rate of ionizing photon production in compact star-forming galaxies during the epoch of reionization.

*Keywords:* galaxies: evolution, galaxies: ISM, supernovae: general, reionization

### 1. INTRODUCTION

Between redshifts  $6 \lesssim z \lesssim 12$ , the Universe underwent a major phase transition from predominantly neutral to fully ionized gas, marking the end of the cosmic dark ages (Fan et al. 2006a; Schroeder et al. 2013; Hinshaw et al. 2013; McGreer et al. 2015; Robertson et al. 2015; Planck Collaboration et al. 2020). Called the Epoch of

Reionization (EoR), this was a critical period in cosmic evolution during which the first galaxies are believed to have been responsible for emitting ionizing radiation and ionizing the neutral intergalactic medium (IGM). However, the mechanisms and topology of reionization remain uncertain, with ongoing debate over the dominant ionizing sources (Madau et al. 1999; Barkana & Loeb 2001; Furlanetto et al. 2004; Dayal & Ferrara 2018), the timing and duration of reionization (Fan et al. 2006b; Becker et al. 2015), and whether the process proceeded in an “inside-out” or “outside-in” manner: two contrasting topologies of ionization that differ in whether

Corresponding author: Miranda Y. Kong  
 ykong2@hawaii.edu

\* NSF Graduate Research Fellow

reionization starts in the densest regions and then expands outward into the low density IGM, or whether it starts in low density voids where recombination rates are low (Furlanetto et al. 2006; Zaroubi 2013; Kimm & Cen 2014; Madau & Haardt 2015; Dayal & Ferrara 2018; Robertson 2022).

Although the exact sources of ionizing photons are still an open question, radiation from low-mass, compact, star-forming galaxies (SFGs) is a popular candidate for satisfying the reionization photon budget and completing reionization by  $z \sim 6$  (Richards et al. 2006; Madau & Dickinson 2014; Robertson et al. 2015; Robertson 2022). Young, hot stars emit Lyman-continuum (LyC) photons with  $\lambda < 912\text{\AA}$ , and therefore enough energy to ionize hydrogen; these photons can escape into the IGM and ionize the surrounding neutral medium. Galaxies that leak a significant fraction of their ionizing photons are, therefore, strong contenders for dominating the ionizing photon budget, as their LyC emission carves out bubbles of ionized hydrogen in the IGM (Finkelstein et al. 2015; Sharma et al. 2016).

Recent theoretical frameworks have proposed various scenarios by which these high- $z$  galaxies might have contributed to cosmic reionization. These scenarios differ in their predictions of which galaxies are most responsible for reionization, and have consequences for the resulting topology of the IGM at high redshift. Two contrasting paradigms include the so-called “democratic” and “oligarchic” models. In the democratic model, either numerous low-mass faint galaxies with modest escape fractions ( $f_{\text{esc}} \sim 10 - 20\%$ ) dominate the ionizing photon budget (Razoumov & Sommer-Larsen 2010; Finkelstein et al. 2015, 2019; Mascia et al. 2024; Rinaldi et al. 2024), or ultra-faint proto-galaxies leak an even larger fraction ( $f_{\text{esc}} \sim 30 - 40\%$ ) of their ionizing photons (Paardekooper et al. 2013, 2015). Alternatively, in the “oligarchic” model, a smaller population of relatively massive early-Universe galaxies —  $M_* \gtrsim 10^{8.5} M_\odot$  — with high  $f_{\text{esc}}$  drive the majority of reionization by carving out large ionizing bubbles (Sharma et al. 2016; Naidu et al. 2020).

Additional scenarios have also been proposed, including (1) AGN feedback models, where quasars and early AGNs are considered a non-negligible source of ionizing photons (Madau et al. 2024), and can constitute  $\sim 10\%$  of the ionizing photon budget (e.g., Dayal et al. 2020); (2) environment-dependent escape fractions, where tidal forces and mergers can significantly change the structure and column density of the interstellar medium (ISM; Madau & Haardt 2015; Dayal et al. 2020; Lewis et al. 2023; Jiang et al. 2025); and (3) intermediate-mass galaxies that sit between the extreme scenarios,

corresponding to a peak far-ultraviolet absolute magnitude ( $M_{\text{FUV}}$ ) at which galaxies contribute the most, with contributions decreasing toward both fainter and brighter  $M_{\text{FUV}}$  (Ma et al. 2020; Matthee et al. 2022; Lin et al. 2024b). It is worth noting that although these models primarily focus on the properties of individual galaxies, protoclusters and groups can also act in tandem to carve out bigger ionized bubbles or induce ionizing AGN activity (Tilvi et al. 2020; Shah et al. 2024).

The LyC escape fractions in high- $z$  SFGs also depend on halo mass, column density, dust production, and ISM geometry (Shapley et al. 2006; Wise & Cen 2009; Wise et al. 2014). The “democratic” scenarios posit that lower-mass galaxies (and thus lower-mass dark matter halos) should have higher Lyman escape fractions due to low gas covering fractions and shallower potential wells, making it easier for ionizing photons to penetrate the ISM. In comparison, massive galaxies and their deeper potential wells form high-density gas reservoirs with column densities that render them effectively opaque to LyC photons (e.g.  $M_{\text{halo}} > 10^8 - 10^9 M_\odot$ , Gnedin et al. 2008; Paardekooper et al. 2013; Kimm & Cen 2014; Finkelstein et al. 2019).

However, mechanical energy injections from feedback can change the galaxy topology. Feedback processes can clear or significantly lower the ISM density, increasing  $f_{\text{esc}}$  (Heckman et al. 2001; Clarke & Oey 2002; Keller & Kruijssen 2022; Flury et al. 2025). Effects from stellar feedback, AGN feedback, SN feedback, and resulting interstellar winds are all proposed as critical sources of mechanical energy that can clear out gas and dust channels through the ISM (Heckman et al. 2011; Amorín et al. 2012; Trebitsch et al. 2017; Nelson et al. 2019; Flury et al. 2022a; Llerena et al. 2023; Jiang et al. 2025). The timeline of these feedback effects is considered to be around 2 – 3 Myr, though the process of clearing out channels can extend up to 10 Myr (Naidu et al. 2022). These time scales, however, remain mainly theoretical and are yet to be directly tested.

Currently, the level at which such feedback processes contribute to reionization is poorly constrained. Studying galaxies during the EoR is difficult because they are so distant. Studying SNe at these redshifts is even more difficult; even with the *James Webb Space Telescope* (*JWST*), the highest redshift SN candidate to date is at  $z = 5.274$  — several hundred Myrs after the canonical end of reionization — and has only a single epoch of observation (DeCoursey et al. 2025). The highest redshift SN confirmed with spectroscopy is at  $z < 4$  (DeCoursey et al. 2024; Coulter et al. 2025). There have also been observations of gamma-ray bursts following a SN candidate at  $z \simeq 7.3$ , deep in the era of reionization,

though without direct SN observations (Cordier et al. 2025; Levan et al. 2025).

Fortunately, a population of galaxies at low redshifts has attributes similar to SFGs during the EoR. High-redshift SFGs are usually compact in size, with low stellar masses, dust extinctions, metallicities, oxygen abundances, and blue UV continuum slopes, but with high emission-line equivalent widths of high-ionization tracers like [O III], and high specific star-formation rates (SFRs; Yang et al. 2017; Izotov et al. 2015, 2021). A population of galaxies in the low-redshift regime, named Green Pea Galaxies (GP) after their optical color in SDSS filters (Cardamone et al. 2009), match these attributes and are commonly considered to be local analogs of high-redshift SFGs (Yang et al. 2016; Kim et al. 2021; Schaefer et al. 2022).

GPs owe their optical colors to extremely high emission line equivalent widths (EWs), especially [O III]  $\lambda 5007$ , and high contrast between their lines and continua. Their high line equivalent widths result from high star formation and the lack of a prominent older stellar population, which together sustain a hard ionizing spectrum and elevated electron temperatures; this leads to particularly strong [O III]  $\lambda 5007$  emission and other high-ionization lines alike (e.g., Ne III; Berg et al. 2012; Jaskot & Oey 2014; Senchyna et al. 2017). At the lowest redshifts — here, we choose  $z < 0.12$  following color selection criteria from Liu et al. 2022 — we refer to these galaxies as “Blueberries” (BBs)<sup>1</sup>, as their [O III] line emission dominates the  $g$ -band (Yang et al. 2016, 2017).

Although observations are not yet powerful enough to detect SNe in EoR galaxies, discovering them in GP and BB galaxies is much more tractable. In recent years, high-cadence all-sky surveys such as the Zwicky Transient Facility (ZTF, Bellm et al. 2019), the Asteroid Terrestrial-impact Last Alert System (ATLAS, Tonry et al. 2018), the ALL-Sky Automated Survey for Supernovae (ASAS-SN, Shappee et al. 2014) and the Panoramic Survey Telescope and Rapid Response System (Pan-STARRS, Chambers et al. 2016), have begun discovering tens of thousands of SNe, particularly at low redshifts ( $z < 0.1$ ) where BB galaxies reside. With future surveys such as the Vera C. Rubin Observatory’s Legacy Survey of Space and Time (LSST; Brough et al. 2020) and the *Roman Space Telescope* high-latitude time-domain survey (Rose et al. 2021, 2025; Observations Time Allocation Committee & Community Survey Definition Committees 2025), the size of the SN sample

will continue to increase through ongoing discoveries, follow-up observations, and classifications.

In this paper, we search for recent SN explosions occurring in two samples of BB galaxies (Jiang et al. 2019; Liu et al. 2022). Our analysis is predicated on the fact that galaxies in which a SN has been directly observed are likely to have higher SN explosion frequencies overall compared to non-host galaxies, while the same types of SNe are found more often in multi-SN hosts (Anderson & Soto 2013). This implies that past SN explosions will have shaped the ISM in these galaxies to a greater degree than non-SN hosts; this is particularly true for CC SNe, whose rates follow the bursty SFHs of these BB galaxies. SN II progenitors, for example, are preceded by the explosions of the more massive SNe Ib and Ic progenitors in the Myr prior to their own terminal explosions.

After selection cuts, we identify 11 SNe in 1242  $z < 0.12$  BB galaxies. Using this sample, we compare SN-host galaxy masses, SFRs, ultraviolet (UV) slopes, and other derived quantities to the larger BB sample and field galaxies as a whole. We infer the relative SN rate for these BB host galaxies, which has implications for how much mechanical energy SNe are injecting into the neutral ISM at high redshifts, and use these derived quantities to better understand the role of SN explosions in allowing LyC escape during the EoR.

In Section 2, we present the BB galaxy samples and SN light curves. We measure relative SN rates and galaxy properties in Sections 3 and 4, respectively. Finally, we discuss implications for cosmic reionization in Section 5. Throughout this study, we use a flat  $\Lambda$ CDM cosmology with  $H_0 = 70 \text{ km s}^{-1} \text{ Mpc}^{-1}$  and  $\Omega_m = 0.3$  for all luminosities and absolute magnitudes, with magnitudes given in the AB system. All SED fitting and scaling relations are based on the Chabrier initial mass function (Chabrier 2003).

## 2. DATA AND METHODS

### 2.1. Green Pea Galaxy Selection

We use two publicly available GP catalogs for a total sample of 2382 galaxies. The first catalog is selected from the Large Sky Area Multi-Object Fiber Spectroscopic Telescope (LAMOST, Luo et al. 2004), and the second is from the Sloan Digital Sky Survey (SDSS, Albareti et al. 2017). We describe the catalogs below, but for more data details and selection methods, see the catalog papers, Jiang et al. (2019) and Liu et al. (2022), respectively. We note that we adopt the Jiang et al. (2019) and Liu et al. (2022) GP identification criteria for each respective sample in this study, and do not at-

<sup>1</sup> We note that the exact redshift range used to define “Blueberry” galaxies varies in the literature.

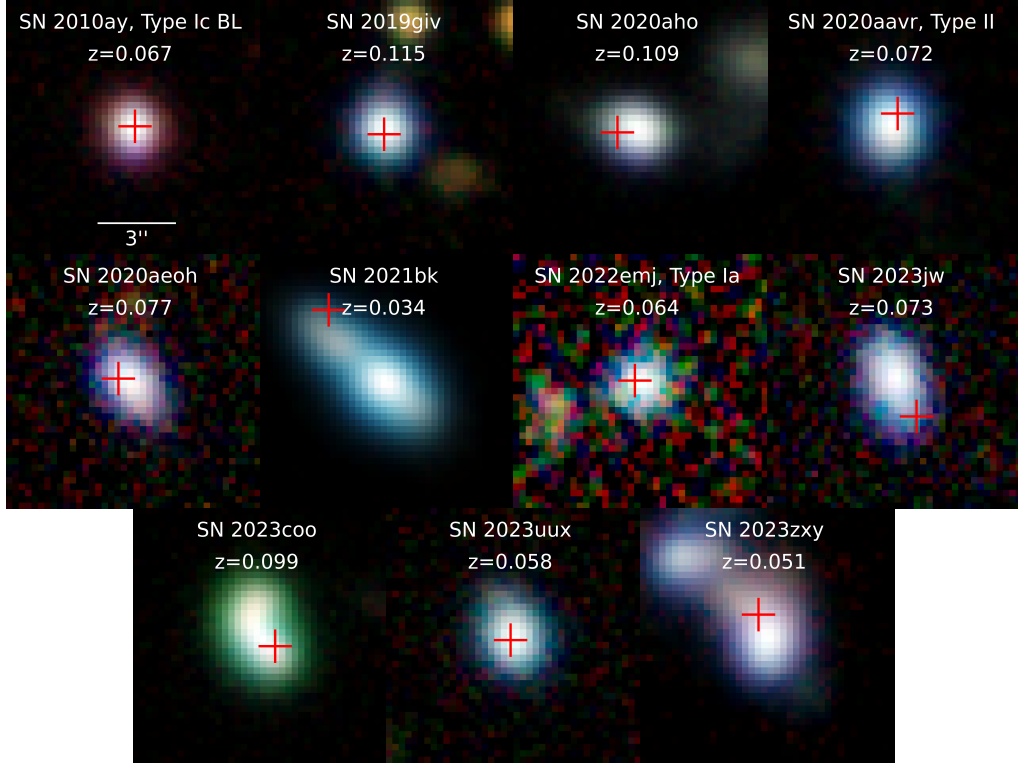


**Figure 1.** Three-color stamp images of the BB SN hosts in our sample, using  $grz$  filters from the DESI Legacy Imaging Survey (Dey et al. 2019; Levi et al. 2019). The images are centered on the host galaxies, while the red crosses mark the coordinates of each SN. Redshifts are derived from SDSS catalogs, which include spectroscopically derived parameters for each host galaxy (York et al. 2000). The scale bar is given in angular size in the top left panel, where 3" corresponds to  $\sim 3$  kpc at  $z = 0.05$  and  $\sim 5.5$  kpc at  $z = 0.1$ . Classification information is from the Transient Name Server (TNS) when available; some SNe in our sample were never spectroscopically classified.

tempt to re-evaluate compactness or color selections to better match EoR galaxies.

LAMOST has carried out spectral observations for millions of stars and galaxies since its commissioning. Its data release (DR) 9 includes 2309 spectra of candidate GP galaxies in the northern sky. From this initial sample, Liu et al. (2022) selected 1547 GP galaxies with strong [OIII]  $\lambda 5007$  emission lines and high equivalent widths, compact physical sizes, and in the redshift range  $0 < z < 0.722$ .

To select GPs, Liu et al. (2022) used a two-fold strategy for the color selection depending on morphology and redshift constraints. For sources in the  $z < 0.12$  range, which is the focus of this work (see Section 2.1.1), they applied loose color criteria with  $u - g \leq 0.3$ ,  $r - g \leq 0.1$ , and  $g - i \leq 0.7$  for extended sources, or strict color criteria with  $u - g \leq 0.5$  and  $r - g \leq 0.5$  when the source had no morphological constraints.

Liu et al. (2022) placed additional constraints on the compactness and line strengths of the color-selected sample, choosing only galaxies with  $r$ -band radii of  $r < 5''$  (at the typical redshift of peas, this corresponds

to an upper limit of  $\sim 5$  kpc in physical half-light radius Cardamone et al. 2009) and an [OIII]  $\lambda 5007$  line flux above  $3 \times 10^{17} \text{ erg s}^{-1} \text{ cm}^{-2}$ .

The second sample comes from a collection of optical spectra of SDSS galaxies from the Baryon Oscillation Spectroscopic Survey (BOSS; Ahn et al. 2014) with corresponding reprocessed Sloan Digital Sky Survey (SDSS; York et al. 2000) legacy survey images. Jiang et al. (2019) selected 835 GP galaxies in the redshift range  $0.011 < z < 0.411$ . The selection criteria requires the galaxies to be spectroscopically classified as a “star-forming”, “starburst”, or “NULL” galaxy subclass (the latter classification denoting that it has no distinct features of any subclass), but not “AGN”. The selection also requires that the [O III]  $\lambda 5007$  and  $H\beta$  lines are detected with a signal-to-noise ratio (S/N)  $> 5$  and have high rest-frame equivalent widths of  $\text{EW}(\text{[O III]} \lambda 5007) > 300\text{\AA}$  or  $\text{EW}(H\beta) > 100\text{\AA}$ , and must be spatially compact with an  $r$ -band radius smaller than 3". They include only those sources that are classified as star-forming galaxies by BPT diagrams, a common tool for classifying galaxies by distinguishing their

Survey	Total Sample	$z < 0.12$ Sample	SN Matches	Reference
LAMOST GP	1694	791	4	Liu et al. (2022)
SDSS GP	1004	482	7	Jiang et al. (2019)
SDSS Field	778 914	311 769	7691	Albareti et al. (2017)

**Table 1.** Sizes of the LAMOST and SDSS GP samples and the SDSS field-galaxy sample. We include the size of the full sample of galaxies and the filtered  $z < 0.12$  subsets, which we address as BB galaxies and their field counterparts in this study.

gas ionization mechanisms (Baldwin et al. 1981). Additionally, the sample chose galaxies with a  $S/N > 3$  for  $[\text{O III}] \lambda 4363$ , though due to its close correlation with  $[\text{O III}] \lambda 5007$ , the effect of this filter is minimal.

We note there are two main differences between the Liu et al. (2022) and Jiang et al. (2019) selection criteria. While Liu et al. (2022) apply strict color criteria based on imaging, the Jiang et al. (2019) sample is primarily determined by line strengths and EWs. Jiang et al. (2019) sets thresholds on both  $[\text{O III}]$  and  $H\beta$ , while Liu et al. (2022) uses only  $[\text{O III}] \lambda 5007$ . Jiang et al. (2019) also applies a tighter cut on spatial compactness of the  $r$ -band radius  $< 3''$ . Additionally, upon visual inspection of a subsample in the optical band, we find that some Liu et al. (2022) GP candidates are bright star-forming knots embedded in larger extended galaxies; however, we found that  $>99\%$  are bona fide GPs, and that this contamination will have a statistically insignificant effect on our SN occurrence rate measurements (Section 3).

Throughout, we use the full SDSS spectroscopic catalog from DR13 as a comparison sample. We filter the catalog to include only “galaxy” type objects, and limit to  $z < 0.12$  to align with the BB sample.

### 2.1.1. Supernova Search

For every galaxy in the BB sample, we perform an initial search for SNe discovered within  $30''$  of their host centers, a radius  $\gtrsim 6 - 10$  times the size of a typical BB galaxy that was chosen to ensure that all SNe associated with a given host can be found. We search through all SNe that have been publicly reported to the International Astronomical Union (via the Transient Name Server<sup>2</sup>). Once we find a possible match, we visually inspect the results to see if the SN is coincident with the galaxy. All of our bona fide SNe were found within  $\sim 2''$  of the host-galaxy center, demonstrating that our conservative initial  $30''$  matching threshold is sufficient for compact galaxies like BBs.

We find 11 SN candidates within close proximity to, and likely hosted by, one of the BB galaxies; an additional 3 are found in the higher-redshift GP sample and are later rejected from our sample due to quality cuts

(see below). The sizes of our samples and the numbers of identified SN hosts are listed in Table 1. All but one of these SNe occurred during the last seven years, due to the recent increase in SN discoveries. The exception is SN 2010ay, a Type Ic-BL SN discovered by Pan-STARRS and published in Sanders et al. (2012). We obtained light curve data from the ZTF, ATLAS, and Pan-STARRS surveys to confirm that the candidates were real SNe and describe these data below.

First, ZTF is a wide-field optical time domain survey that scans the entire Northern sky in the  $g$ ,  $r$ , and  $i$  filters. We obtained ZTF data using the publicly available ZTF forced photometry service (Masci et al. 2019), which allows users to request forced-photometry lightcurves at any coordinate on the sky.

ATLAS consists of four telescopes in Hawai‘i (Maunaloa and Haleakalā), Chile, and South Africa, which scan the whole sky several times each night in the cyan and orange broadband filters (equivalent to  $g + r$  and  $r + i$ , approximately). We obtained these data using their forced-photometry service (Shingles et al. 2021).<sup>3</sup>

The Pan-STARRS telescopes also provide wide-field imaging of the night sky in  $griz$  filters. Photometry is provided by the Pan-STARRS image processing pipeline (IPP) at the University of Hawai‘i; the IPP performs data processing, calibration, difference imaging, and photometry for all Pan-STARRS data (Flewelling et al. 2020; Magnier et al. 2020). Data are passed to a version of the Transient Science Server (Smith et al. 2020), which carries out searches for new SNe as part of the Pan-STARRS Survey for Transients (PSST, Huber et al. 2015). Once a candidate SN is discovered, forced photometry is automatically carried out at the location of the SN.

We constructed light curves using the available photometry with all 14 SNe, as shown in Figure 2. We note that SN 2010ay predates the start of the ZTF and ATLAS surveys, hence we were only able to retrieve Pan-STARRS photometry; we additionally compiled synthetic photometry and Gemini/GMOS data from Sanders et al. (2012) as part of Figure 2.

<sup>3</sup> <https://fallingstar-data.com/forcedphot/>.

<sup>2</sup> <https://www.wis-tns.org/>.

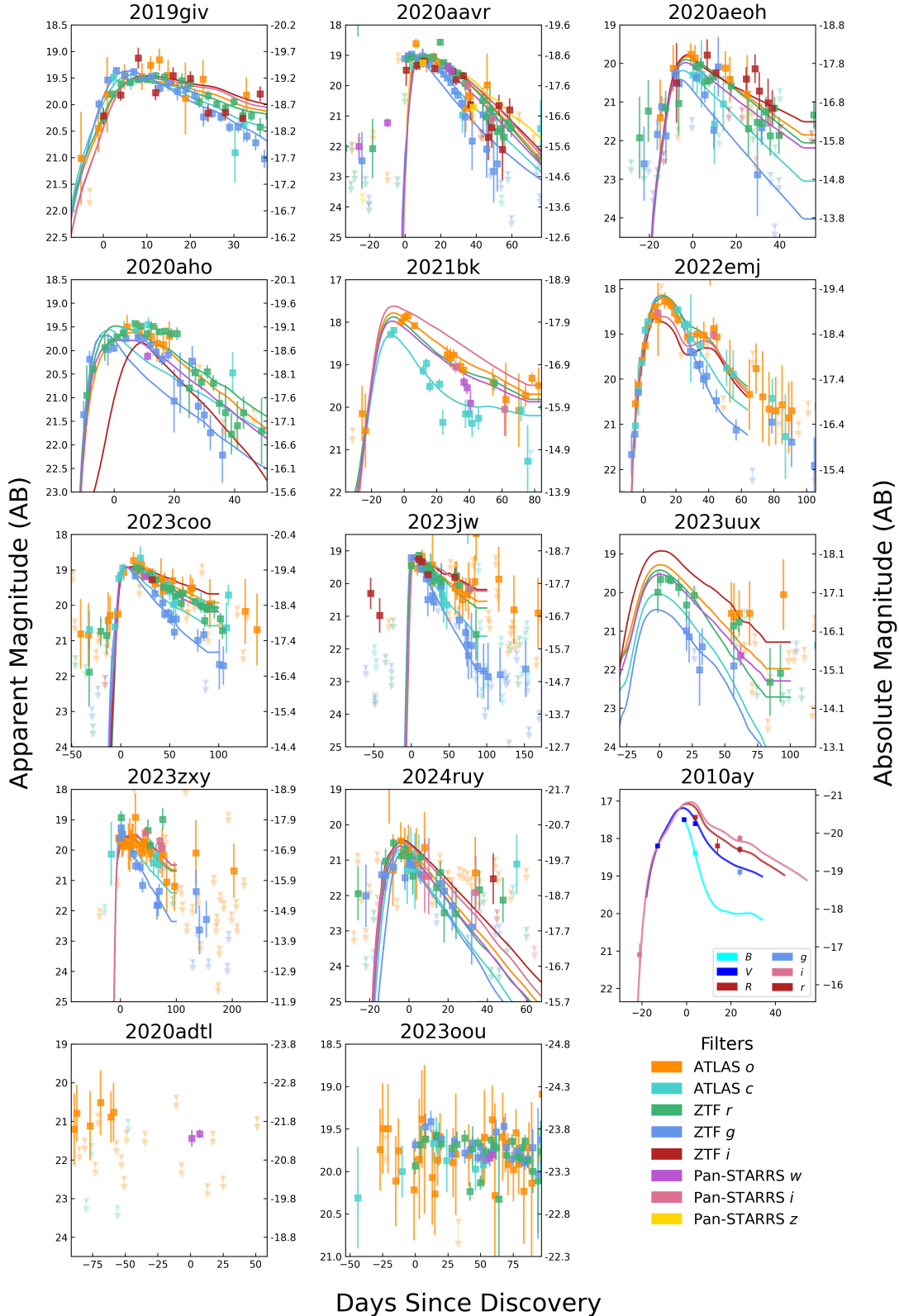


**Figure 2.** ZTF, ATLAS, and Pan-STARRS light curves for all SNe in our matched sample, with SN 2010ay from Sanders et al. (2012) including synthetic photometry from Gemini observations. SN candidates 2024ruy, 2020adtl, and 2023ouu are excluded from our analysis. We show the best-fit STARDUST2 model for each bona fide SN (Rodney et al. 2014).

Upon visual inspection and redshift filtering, we remove three of the 14 candidates from the sample. Two (2020adtl and 2023oou) are identified as QSO objects by SDSS; they also do not appear to have a clear monotonic rise or fall in their light curves, and therefore are likely not real SNe. Furthermore, they both have redshifts of  $z > 0.6$ ; typical SNe at these redshifts would be well below the detection threshold of ATLAS, ZTF, or Pan-STARRS. One additional SN candidate, SN 2024ruy, has a redshift of 0.26, higher than the rest of the SNe hosts and the local BB population; it is removed to limit our BB sample to  $z < 0.12$ , which also preserves consistency in color selection with the LAMOST sample.

After selection cuts, our final sample includes four SNe in the LAMOST galaxies, and seven in the SDSS galaxies, for a total of 11 SNe. Detailed information for these SNe and their hosts is listed in Table 2. Three SNe were classified spectroscopically: 2010ay as Type Ic-BL, 2020aavr as Type II, and 2022emj as Type Ia. These 11 SNe are considered to be our final sample of BB-hosted SNe and the main subject of study for this paper.

We also cross-match TNS objects to field galaxies to use as a comparison sample, first filtering the field galaxies to match the redshift range of the BB SN hosts ( $z < 0.12$ ). This gives the field-galaxy sample comparable selection effects (i.e., Malmquist bias) to the BB sample. For these galaxies, we conservatively perform a cone search for SNe within a  $75''$  radius of each host galaxy center. We then keep only those SNe for which the galaxy is the most probable host, as determined by the GHOST algorithm (Gagliano et al. 2021); GHOST finds the most likely host galaxy for each SN by using a gradient ascent algorithm trained on the Pan-STARRS photometric catalog. This cross match yields a total of 7691 SNe from our sample of 311 769 SDSS field galaxies.

## 2.2. Supernova Classifications

For those SNe lacking spectroscopic classifications, we use their peak luminosities, model fits with the SALT3 SN Ia standardization model (Kenworthy et al. 2021), and the STARDUST2 classifier (Rodney et al. 2014) to derive approximate SN types. Our primary classifier is STARDUST2, a Bayesian classifier originally built for high-redshift SNe discovered by the *Hubble Space Telescope* (*HST*), which compares the data to simulated SN light curves from 27 Type II and 15 Type Ib/c templates, as well as the SALT3 SN Ia model (Kenworthy et al. 2021; Pierel et al. 2022). Realistic luminosity and dust distributions are applied to the templates, with additional details provided in Rodney et al. (2014); DeCoursey et al. (2024). The number of simulated samples for each SN

type is scaled by the volumetric rates from Dilday et al. (2008) and Li et al. (2011). From these simulations, STARDUST2 then marginalizes over the probability that a SN is Type Ia, Ib/c, or II. For samples with limited data, such as ours, the strength of STARDUST is that it does not require a large sample of simulated or real light curves to train a machine-learning algorithm.

From just peak magnitudes alone, we find that four of eight unclassified SNe are likely CCSNe; from Desai et al. (2024, their Table 1 at  $z > 0.02$ ), the mean absolute magnitude of SNe Ia in a magnitude-limited sample is approximately  $V \simeq -19.05 \pm 0.44$  mag. This is strongly inconsistent with the observed luminosities of SNe 2023uux and 2023zxy, which STARDUST2 classifies as SNe Ib/c and II, respectively. SNe 2021bk and 2020aeoh have a  $<3\%$  chance of being SNe Ia; STARDUST2 classifies both as SNe Ib/c.

For the remaining SNe, we use the SALT3 model (Kenworthy et al. 2021) as implemented in `sncosmo` (Barbary et al. 2016) to determine whether the best-fit light curves are consistent with a SN Ia. We find that SN 2019giv rises to peak approximately twice as fast ( $\sim 8$  days) as would be expected for its best-fit stretch; accordingly, STARDUST2 classifies it as a SN II. SN 2020aho's luminosity is consistent with a SN Ia, and STARDUST2 classifies it as a SN Ia, but the SALT3 fit shows inconsistent early versus late-time colors between data and model, as well as a prominent bump in the early-time  $g$ -band light curve that indicates shock breakout characteristic of a SN II (some SNe Ia have early time excesses, but typically they occur at several mag below peak; Hoogendam et al. 2024). SN 2023jw is somewhat underluminous for a SN Ia, and its best-fit shape ( $x_1$ ) and color ( $c$ ) parameters are inconsistent with a SN Ia (too high-stretch and red, respectively); STARDUST2 classifies it as a SN II. Lastly, SN 2023coo declines too slowly to be a SN Ia, and STARDUST2 classifies it as another SN II.

Overall, we find that the SNe in our sample, with the exception of SN 2022emj, are likely to be CCSNe. This means that they should probe the star-forming environment of their host galaxies within the last  $\sim 10\text{--}50$  Myr (Zapartas et al. 2017). We note that our sample has a high fraction of core-collapse SNe when compared to the field, though we do not further probe the characteristics of these SNe in this work.

## 3. RELATIVE OCCURRENCE RATES OF SUPERNOVAE IN BLUEBERRY GALAXIES

Understanding how frequently SNe occur in different galaxy environments provides insight into the nature of their stellar populations and the feedback processes

SN ID	Host Survey	Host ID	Host z	Spec. Class.	Abs. Mag.
2010ay	LAMOST	SDSS J123527.19+270402.7	0.0671	Ic-BL	-20.2
2023uux	LAMOST	SDSS J104040.26+055405.9	0.0577	...	-17.4
2020aeoh	LAMOST	SDSS J100741.62+082536.4	0.0767	...	-18.2
2023jw	LAMOST	SDSS J123154.45+313707.6	0.0730	...	-18.6
2020aavr	SDSS	SDSS J085949.12+380632.1	0.0725	II	-18.6
2020aho	SDSS	SDSS J082722.57+202612.8	0.1086	...	-19.2
2023zxy	SDSS	SDSS J122611.15+532602.0	0.0514	...	-17.9
2022emj	SDSS	SDSS J121234.81+463541.2	0.0643	Ia	-19.3
2019giv	SDSS	SDSS J154659.01+325632.2	0.1148	...	-19.5
2021bk	SDSS	SDSS J135950.91+572622.9	0.0338	...	-18.1
2023coo	SDSS	SDSS J112145.16-000121.2	0.0990	...	-19.7

**Table 2.** BB-hosted SNe, including their respective hosts, redshifts, spectroscopic classifications, and approximate absolute magnitudes at peak. The absolute magnitude for 2010ay is taken from [Sanders et al. \(2012\)](#), while all others are measured from our lightcurve data. SN 2010ay, 2020aavr, and 2022emj are spectroscopically classified. The unclassified SNe are likely core-collapse SNe, which we determine using photometric classification in Section 2.2.

that regulate galaxy evolution. In particular, the rate of CC SNe is closely tied to recent star formation, reflecting the short lifetimes of massive progenitor stars ([Mannucci et al. 2005](#); [Kennicutt & Evans 2012](#); [Strolger et al. 2015](#)). To evaluate whether the compact star-forming environment of BB galaxies has a measurable effect on the SN rate, we estimate the relative frequency of CCSNe in 1242 BB galaxies (SDSS and LAMOST combined) and compare this sample to the redshift-matched field sample.

We first derive approximate host-galaxy masses and SFRs from scaling relations relying on optical and UV photometry. These allow us to quickly measure SED properties across more than  $10^6$  galaxies, providing a determination of SN rates from the field-galaxy sample as a function of those properties. We obtain GALEX and SDSS photometry for the full BB and SDSS field-galaxy sample at  $z < 0.12$  by querying their respective catalogs. All galaxies have spectroscopic redshifts for determining estimated distance moduli, used to measure absolute magnitudes.

We measure the mass using the scaling relation provided by [Taylor et al. \(2011\)](#), their Equation 8), which is based on SDSS *gi* magnitudes. To validate these masses, we compare them to SDSS catalog mass measurements, which use the spectroscopically derived redshifts and *ugriz* photometry ([Maraston et al. 2013](#)), for a subset of our sample. This comparison yields a statistically significant correlation coefficient of 0.728, a mean offset of 0.06 dex, and a scatter of 0.63 dex; scatter is dominated by the low-mass end, and is likely due to the breakdown of color–M/L calibrations in emission-line dominated SFGs ([Roediger & Courteau 2015](#); [Sorba & Sawicki 2015](#)). We also note that both mass measurements assume parametric star-formation histories,

which can cause stellar masses to be underestimated by  $\sim$ 0.1–0.2 dex ([Leja et al. 2019](#)).

We also specifically examine the low-mass range of this comparison, finding slightly higher scatter of  $\sim$ 0.8 dex between  $6 < \log(M_*/M_\odot) < 7$ . Because BB SNe have high [OIII] flux in the *g* band, it is possible that this band is line-dominated; this effect would systematically reduce the [Taylor et al. \(2011\)](#) mass estimates by changing the color correction term. However, we see that the [Taylor et al. \(2011\)](#) masses are generally higher (by  $\sim$ 0.4 dex) than the SDSS spectroscopic measurements for these low-mass data (but with significant scatter).

Our SFR measurement uses the relationship from [Salim et al. \(2007\)](#), see also [Rigault et al. 2015](#)) derived from GALEX *FUV* magnitudes ([Martin et al. 2005](#)). The dust-corrected UV emission of galaxies redward of the LyC break directly traces the emission of relatively young stars, and is therefore a good tracer of SFR on  $\sim$ 100 Myr timescales ([Flores Velázquez et al. 2021](#)). We correct for Milky Way extinction using the [Schlegel et al. \(1998\)](#) reddening maps, the [Schlafly & Finkbeiner \(2011\)](#) dust temperature correction, and a reddening law of  $R_V = 3.1$ . We approximately correct for the galaxy extinction,  $A_{FUV}$ , using *FUV*–*NUV* colors following [Rigault et al. \(2015\)](#), and convert to *FUV* luminosity using the distance modulus. We then use the relationship from [Kennicutt & Evans \(2012\)](#) to infer the time-delayed SFR from the dust-corrected *FUV* luminosities:

$$\log \left( \frac{SFR}{M_\odot \text{ yr}^{-1}} \right) = 1.2 \times 10^{-28} L_{\nu, FUV} \text{ (erg/s/Hz)}. \quad (1)$$

We again compare these calculations to SDSS spectroscopically derived measurements, and find a statistically significant linear correlation with a coefficient of 0.76

and a standard deviation of 0.44 dex. We note that the SDSS fiber diameter (2–3'') might not cover the full region of more extended field galaxies — and preferentially include older stellar populations near the galaxy center — and therefore underestimate their SFR, which is less of a concern for compact BB galaxies, resulting in subtle biases in this comparison.

### 3.1. Results

In Figures 3 and 4, we show the fraction of galaxies hosting SNe, for both BB and field galaxies, binned by mass and SFR respectively. Because we wish to specifically study the rate of CCSNe, we include only likely CCSNe in the BB sample (all SNe except for SN 2022emj). We also include only classified CCSNe in the field galaxy sample, but correct their measured rates by the overall classification fraction of SNe hosted by  $z < 0.12$  SDSS galaxies ( $\sim 25\%$ ) so that we can fairly compare these relative rates to the photometrically classified BB SN sample.

Compared to the full field galaxy sample at stellar masses  $< 10$  dex — to limit to the mass range where BB galaxies are found — BBs show lower SN frequency; approximately  $0.9 \pm 0.3\%$  of BB galaxies in our sample were observed to host CCSNe, while  $1.5 \pm 0.1\%$  of field galaxies hosted CCSNe after correcting for the classification incompleteness as described above. The difference in frequency is  $\Delta f = 0.59 \pm 0.29\%$ , significant at the  $2.1\sigma$  level. However, the field galaxies overall have higher masses than the BB sample; when we require a mass limit such that the median mass of the BB sample is the same as that of the field sample, we find a less confident  $\Delta f = 0.46 \pm 0.37\%$  ( $1.2\sigma$ ). There is also some potential for systematic bias in our mass calculations at the lowest masses, as discussed above, which could reduce the significance of this difference further.

Additionally, the subset of galaxies for which GALEX *FUV* measurements are available show a slightly *higher* SN rate in the BB galaxies than the field sample ( $1.0 \pm 0.05\%$  for the field versus  $1.1 \pm 0.3\%$  for the BB sample). However, because only 1/10 BB-hosted CC SNe have unreliable GALEX *FUV* data, while 34% of the field sample is missing *FUV* data, we consider this result to be dominated by statistical fluctuation.

In Figure 3, we show the relative frequency of SNe as a function of mass in BBs, all SDSS field galaxies, and field SFGs. To isolate the SFG sample, we select galaxies with  $u - r < 2.3$  mag, which follows the bimodal distribution of the  $u - r$  color in our sample. We note that this color cut excludes both quiescent galaxies and dusty star-forming galaxies (DSFGs), which are predominantly bright in the mid-to-far infrared. (Blain

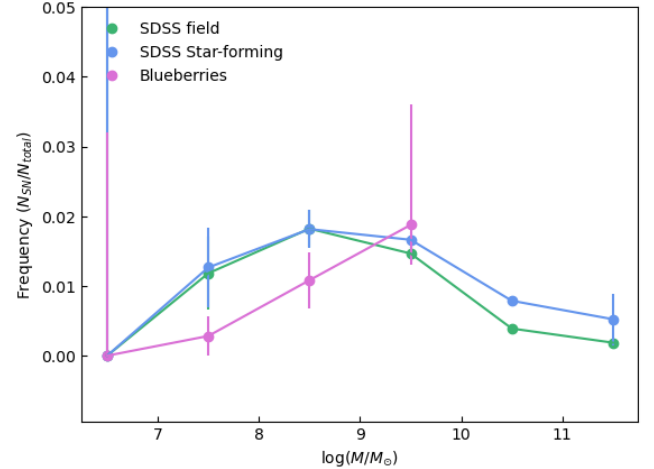


**Figure 3.** SN event frequency ( $N_{\text{SN}}/N_{\text{total}}$ ) as a function of mass for the SDSS field galaxy sample (green), the color-filtered SFG sample (blue), and the BB sample (pink). Error bars are derived from Poisson statistics for galaxies in the given stellar mass bin. The BB sample shows a lower frequency of SN events.

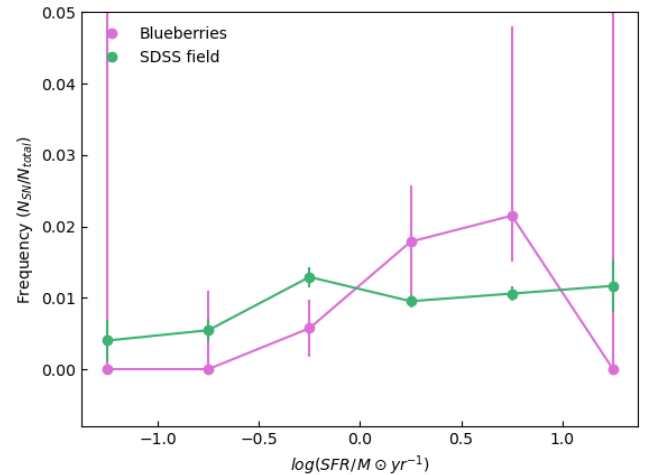


**Figure 4.** SN frequency for the SDSS field galaxy sample (green) and the BB sample (pink). Each sample is binned by FUV-calculated SFR, and frequency is calculated by  $N_{\text{SN}}/N_{\text{total}}$  in each bin. See the Figure 3 caption for additional details.

et al. 2002; Chapman et al. 2005; Casey et al. 2014; Bussmann et al. 2015). This filter yields 139 430 SFGs. We see largely consistent rates between all field galaxies and field SFGs at masses  $< 10$  dex, which is unsurprising given that most of these galaxies are star-forming; at higher masses, the difference between the overall field rates and the SFG rates reflect the higher fraction of passive galaxies at these masses, which do not host CCSNe.

Both Figures 3 and 4 show that BB galaxies tend to have a lower rate of SN occurrence compared to the field

galaxies in the low mass and low SFR bins (at  $\sim 2\sigma$  significance), while at high mass and SFR the rates are comparable. In addition to the caveats above, however, we also note that SNe in BB galaxies may be systematically under-reported, which may be due to their host galaxies being mistaken for high-redshift AGN, and would cause their rate to be higher than calculated in this study. In future work, we plan to perform a more exhaustive forced-photometry search for previously undetected BB-hosted SNe, with surveys such as Pan-STARRS and ZTF. We discuss the potential implications of low SN rates in BB galaxies in Section 5.

#### 4. HOST PROPERTIES

The role of SNe in shaping galaxy-scale environments can be traced by the physical conditions of their host galaxies. In this section, we explore whether BB galaxies that host SNe differ systematically from the broader BB sample. In Section 4.1, we investigate the correlation between the presence of SNe and the galaxy stellar mass, SFR, and metallicity; in Section 4.2, we dive deeper into the galaxies’ UV slopes and the implied Lyman continuum escape fractions, while in Section 4.4 we measure the star formation histories of these galaxies.

##### 4.1. Comparing SED Parameters Derived from Spectroscopy

The SDSS BB sample is from DR13, which includes an abundance of spectral property measurements. Redshifts and spectral features are first determined by the SDSS spectroscopic pipeline (Stoughton et al. 2002; Albareti et al. 2017). Subsequently, objects classified as ‘galaxy’ are fitted with stellar population models to derive properties such as star formation rates, stellar masses, and metallicities (Chen et al. 2012; Maraston et al. 2013; Thomas et al. 2013).

In Figure 5, we compare several intrinsic properties of the SN host galaxies to the full SDSS BB sample, which were assembled from the SDSS catalog by Jiang et al. (2019). We measure the difference between SN hosts and the broader BB population using several key physical parameters that are relevant to the production of ionizing photons in SFGs. These include the  $H\alpha$ -derived SFR, the [O/H] metallicity, the SDSS-derived stellar mass from Maraston et al. (2013), and the electron density from the flux ratio  $R \equiv [SII]\lambda 6716/[SII]\lambda 6731$  (Jiang et al. 2019).

We find that non-Ia host galaxies tend to have higher SFR and stellar mass than the non-host BB population, with Kolmogorov–Smirnov (KS) statistics of 0.63 and 0.55, respectively, corresponding to p values of 0.03 and 0.08. We also find offsets of  $3.7\sigma$  (SFR) and  $2.5\sigma$  (mass)

significance in the difference between sample means (we note that we neglect modeling uncertainties in deriving these significances, assuming them to be subdominant).

In contrast, the distributions of electron density and metallicity show no significant differences, with offsets at the  $< 1\sigma$  level. The elevated  $H\alpha$ -derived SFRs of the SN hosts are consistent with expectations that CC SNe form from short-lived, massive stars and therefore occur preferentially in star-forming environments. The shift toward higher stellar masses among SN hosts is likely due to the increase in size of the overall stellar population, meaning that more massive stars exist that can potentially explode as SNe, though higher stellar mass is also generally correlated with higher SFR in SFGs.

Though not included in our significance calculations, we also plot the SNe Ia host galaxy in Figure 5, which does not follow many of these trends. Due to the much longer delay times between star formation and explosion for many SNe Ia (Dilday et al. 2008; Maoz et al. 2014; Keller & Kruijssen 2022), it is not surprising that weaker or different correlations between SNe Ia and galaxy properties may exist (e.g., Nugent et al. 2026).

##### 4.2. UV Slopes

The UV spectral slope (usually measured within the window from  $\sim 1300$  –  $2500$  Å; Calzetti et al. 1994),  $\beta$ , is a tracer of both stellar age and dust content in SFGs (Reddy et al. 2015; Chisholm et al. 2022). Its strong correlation with the LyC escape fraction,  $f_{\text{esc}, \text{LyC}}$ , is both theoretically predicted and demonstrated with data from studies such as the Low-Redshift Lyman Continuum Survey data (LzLCS, Flury et al. 2022b; Zackrisson et al. 2013; Saldana-Lopez et al. 2022; Chisholm et al. 2022).

We compute  $\beta$  using Milky Way extinction-corrected GALEX  $FUV$  and  $NUV$  magnitudes for all BB and GP samples following Equation 1 of Lin et al. (2025, see also Equation 1 of Rogers et al. 2013), which computes the slope from the photometric color:

$$\beta = -0.4 \frac{m_1 - m_2}{\log_{10}(\lambda_1/\lambda_2)} - 2, \quad (2)$$

where we use the corresponding filter pivot wavelengths  $\lambda_{NUV} = 2301$  Å, and  $\lambda_{FUV} = 1535$  Å.

As a consistency check, we also compute  $\beta$  using the SDSS  $u$  and GALEX  $NUV$  colors, and find good agreement with the mean  $\beta$  for the BB sample.<sup>4</sup> Between  $\beta_{FUV-NUV}$  and  $\beta_{NUV-u}$ , we measure a median absolute deviation that is consistent with the errors (i.e.,

<sup>4</sup> We use the subscript notations  $\beta_{FUV-NUV}$  for GALEX color and  $\beta_{NUV-u}$  for the combination of GALEX  $NUV$  and SDSS  $u$  band color.

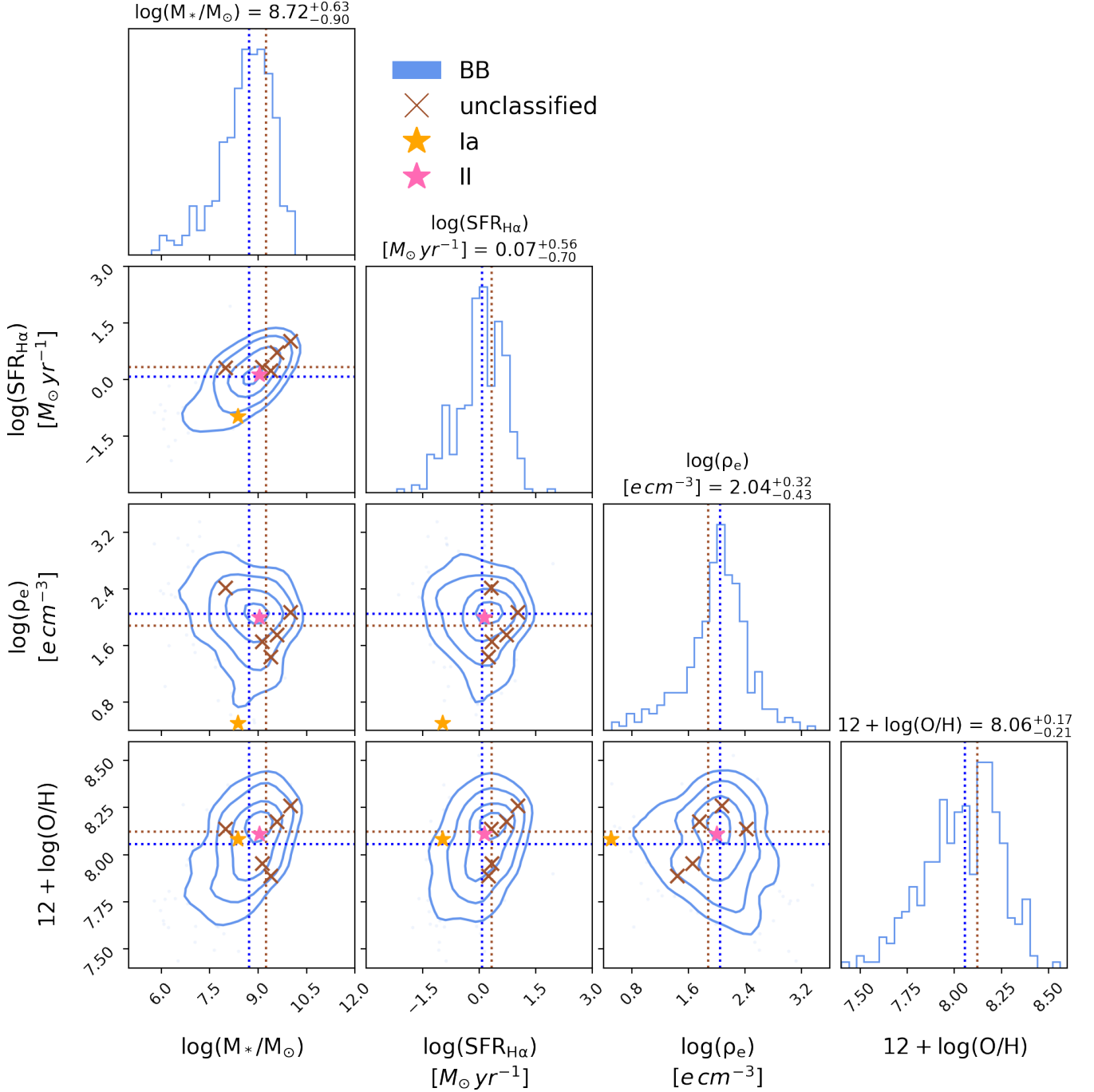


**Figure 5.** Corner plot showing galaxy properties of BB galaxies and BB SN hosts, measured from the SDSS spectroscopic pipeline. Properties include the H $\alpha$ -inferred SFR, electron density, metallicity, and stellar mass. The contours displayed correspond to the 0.5, 1, 1.5, 2 $\sigma$  levels. The unclassified SNe are marked with brown “x” markers, while the classified Type Ia and Type II SNe are marked with orange and pink stars, respectively. Dotted lines represent the population means. Top labels give the medians of each property for the BB galaxies, with error bars corresponding to the 16th and 84th percentiles.

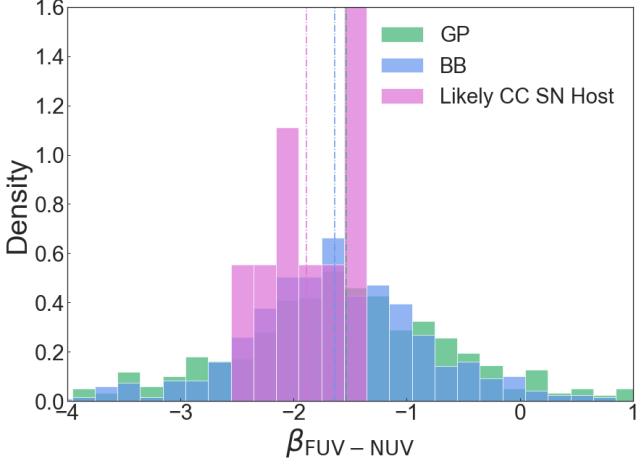


**Figure 6.** The UV slope,  $\beta$ , for GPs (green), BBs (blue), and BB SN hosts (pink). The mean UV slope of SN hosts is lower than that of other BBs at  $2.1\sigma$  significance. SN 2022emj (SN Ia) and SN 2020aho (blended photometry) are excluded from this figure.

a scatter of 0.275 after restricting the sample to  $\beta_{\text{obs}}$  errors on GALEX and SDSS to  $<0.2$ ). However, the SDSS  $u$ -band measurements are more uncertain as a whole, and for lower-redshift SNe ( $z \lesssim 0.05$ ) they are potentially contaminated by [O II] $\lambda 3727$  and  $\lambda 3729$  line flux (GALEX  $FUV$  may also be slightly contaminated by Ly $\alpha$  at  $z > 0.11$  but Ly $\alpha$  would be at the very edge of the  $FUV$  bandpass where sensitivity is lower). For this reason, we use the GALEX-computed  $\beta_{FUV-NUV}$  slopes for this analysis.

We compare the distribution of  $\beta$  between the BBs, GPs, and the SN hosts in Figure 6, and find that SN hosts show a lower mean UV slope,  $\beta_{FUV-NUV} = -1.88$  (median of  $-1.89$ ), than the BB galaxies, which have an average slope of  $-1.63$  (median of  $-1.64$ ). The slopes differ at  $2.1\sigma$  significance, which we compute using the mean and standard error of the populations. We exclude the SN Ia from these calculations, due to its long delay time, as well as SN 2020aho due to substantial blending in GALEX filters with a nearby (and possibly interacting) companion galaxy.

In Figure 7, we compare  $\beta$  to the GALEX  $FUV$  absolute magnitude,  $M_{FUV}$ . We overplot the median linear relationship between  $\beta$  and  $M_{FUV}$ , fitted by Bouwens et al. (2014) for  $z = 2.5$  and  $z = 7.0$ . Although we do not observe any clear trends in the GP and BB populations, the SN host galaxies (pink) loosely follow the empirical relation of Bouwens et al. (2014) and trend toward higher escape fractions for fainter host galaxies, though with significant scatter.

Because  $\beta$  scales strongly with  $f_{\text{esc,LyC}}$ , we can also use the analytic relation proposed by Chisholm et al.

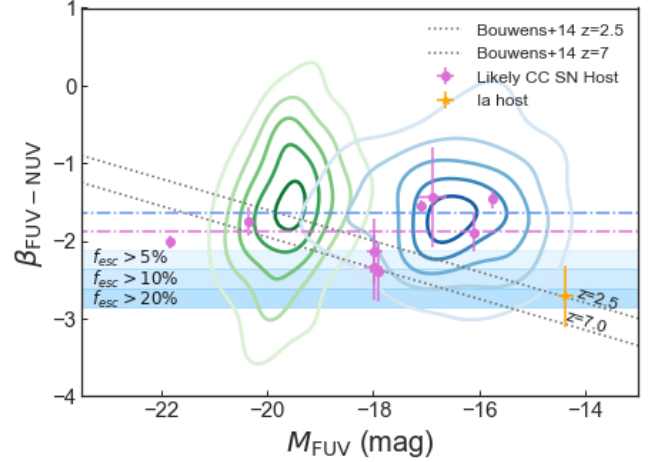


**Figure 7.** The  $\beta$  parameter versus  $FUV$  magnitude ( $M_{FUV}$ ) for GPs (green), BBs (blue), BB SN hosts (core-collapse, pink), and BB Type Ia host (orange star). SN 2020aho (blended photometry) is excluded from this figure. Estimated 5%, 10%, and 20% LyC escape fractions are plotted using Equation 11 from Chisholm et al. (2022). The best-fit  $\beta$  versus  $M_{FUV}$  relationships from Bouwens et al. (2014) at  $z = 2.5$  and  $z = 7$  (grey dotted) are also shown, though we note that many BBs are significantly more UV-faint than the samples in this work.

(2022) to convert  $\beta$  to an approximate LyC escape fraction:

$$f_{\text{esc,LyC}} = (1.3 \pm 0.6) \times 10^{-4} \times 10^{(-1.22 \pm 0.1)\beta}. \quad (3)$$

We note that Chisholm et al. (2022) fit for their UV continuum slope in the  $1300 - 1800\text{\AA}$  wavelength range, while the GALEX  $NUV$  filter extends redder, with an effective wavelength of  $\sim 2300\text{\AA}$ . Raiter et al. (2010) show that measuring  $\beta$  from  $1800 - 2200\text{\AA}$  yields a higher  $\beta$  measurement by  $\sim 0.2 - 0.3$  mag, and depends on the initial mass function and metallicity; however, in this work, the difference in  $\beta$  compared to Chisholm et al. (2022) is likely a more subtle  $\sim 0.1 - 0.15$  mag given that GALEX filters span a wide wavelength range from  $\sim 1500 - 2300\text{\AA}$ .

Using this relation, we shade regions of Figure 7 that correspond to escape fractions of  $> 5\%$ ,  $> 10\%$ , and  $20\% < f_{\text{esc,LyC}} < 40\%$ . These show the number of GP/BB galaxies that are considered “cosmologically relevant” ( $> 5\%$ ) as defined in Chisholm et al. (2022). We identify at least three out of ten CCSN hosts as likely having  $f_{\text{esc}} > 5\%$ . The host of the Type Ia SN (2022emj) may also have a LyC escape fraction of  $\sim 20\%$ .

Additionally, to assess whether the UV-slope distribution of the BB galaxies still differs from that of the SN hosts when controlling for the absolute UV magnitude of each galaxy — given that SN hosts are brighter on average — we perform a bootstrap test. We draw

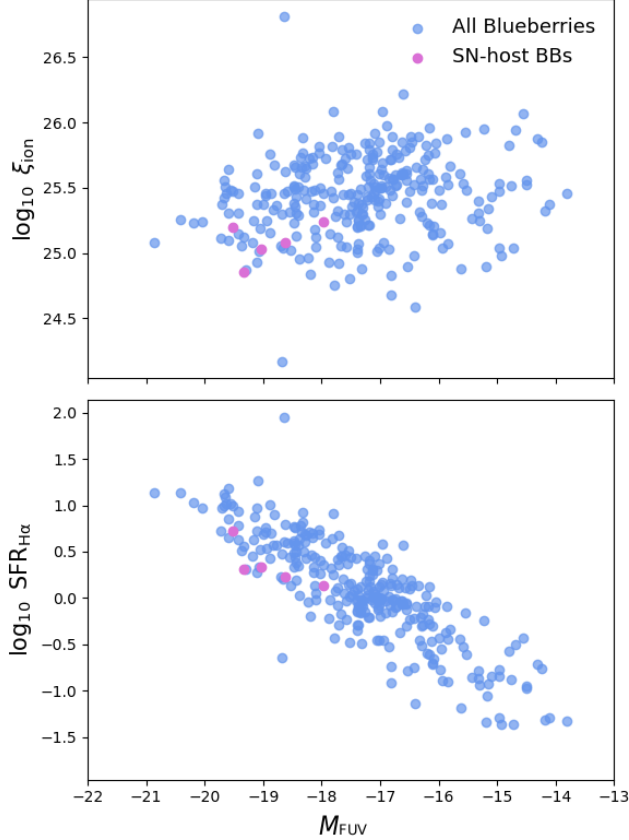


**Figure 8.** Comparisons between  $\xi_{\text{ion}}$ , H $\alpha$ -derived SFR, and FUV absolute magnitude for the SDSS BB sample (blue) and the SDSS SN-hosts (pink), excluding the host of the Type Ia SN 2022emj. The SN hosts have lower than average  $\xi_{\text{ion}}$  (top panel) due to their lower SFR when compared to BB galaxies with similar UV magnitudes (bottom panel).

10 000 random subsamples of 10 non-host BB galaxies, each matched in  $M_{\text{UV}}$  to one of the SN-host galaxies. For each resample, we compute the median UV slope and compare it to that of the SN-host sample. Approximately 10% of the resamples attain a median bluer than  $-1.89$ , the median UV slope of the SN-host galaxies. The average of the resampled medians is  $-1.632$ .

#### 4.3. Ionizing Photon Production

The rate of ionizing photons leaked into the IGM for a given galaxy,  $\Gamma$ , is determined by both the fraction of ionizing photons that escape into the IGM ( $f_{\text{esc}}$ ) and the ionizing photon production efficiency  $\xi_{\text{ion}}$  (Emami et al. 2020):

$$\Gamma = \int L \Phi(L) \xi_{\text{ion}}(L) f_{\text{esc}}(L) dL. \quad (4)$$

Here,  $L$  is the galaxy luminosity and  $\Phi(L)$  denotes the galaxy luminosity function. In SFGs, the values of  $\xi_{\text{ion}}$  and  $f_{\text{esc}}$  can vary substantially depending on internal

conditions such as ISM geometry and density structure (Fernandez & Shull 2011; Rinaldi et al. 2024).

To quantify these properties in our samples, we compute  $L_{H\alpha}$  using the SDSS  $H\alpha$ -derived SFR from (Kennicutt et al. 1994) and use it to estimate  $\xi_{\text{ion}}$  following Emami et al. (2020):

$$\text{SFR}(\text{total}) = \frac{L_{H\alpha}}{1.26 \times 10^{41} \text{ erg s}^{-1}} M_{\odot} \text{ yr}^{-1}, \quad (5)$$

$$\xi_{\text{ion}} = \frac{L_{H\alpha}}{1.36 \times 10^{-12} L_{\text{UV}}} [\text{s}^{-1} / \text{erg s}^{-1} \text{ Hz}^{-1}]. \quad (6)$$

Figure 8 shows  $\xi_{\text{ion}}$  and the  $H\alpha$ -derived SFR as a function of FUV absolute magnitude for the subset of our CCSN hosts and BB galaxies with available SDSS  $H\alpha$  measurements. SN hosts tend to have brighter FUV magnitudes overall, which generally correspond to slightly lower  $\xi_{\text{ion}}$ ; additionally, SN hosts appear to have lower  $H\alpha$ -derived SFR compared to other BBs of similar magnitude. Compared to the full BB sample, we find that SN hosts exhibit lower  $\xi_{\text{ion}}$  values at  $7.9\sigma$  significance.

We then apply the same bootstrap procedure used for  $\beta$  in Section 4.2 to our  $\xi_{\text{ion}}$  measurements to see whether SN hosts have lower  $\xi_{\text{ion}}$  when controlling for their FUV absolute magnitudes. Using 10 000 resamples of the BB population (each matched in size and UV magnitude to the SN-host sample), we find that only 2% yield a median  $\xi_{\text{ion}}$  lower than that of the SN host galaxies.

To further understand the ionizing conditions of these populations, we also compare their [O III]/[O II] ratio ( $[\text{O III}]\lambda\lambda 4959, 5007 / [\text{O II}]\lambda\lambda 3726, 3729$ ), again using SDSS measurements. This is considered one of the optical diagnostics for the hard radiation content and ISM conditions, therefore providing additional information on the total production of ionizing photons (Jaskot & Oey 2014; Nakajima & Ouchi 2014; Izotov et al. 2016a; Ma et al. 2016, 2020). We find a SN hosts may have a lower O32 ratio at  $1.8\sigma$  significance, consistent with our measurements of lower  $\xi_{\text{ion}}$ .

Overall, we note that the statistical significance of some of these differences is marginal given the small sample size; however, our finding that CCSN feedback predominantly occurs in UV-bright galaxies, and that these galaxies have lower  $\xi_{\text{ion}}$  (by approximately  $\sim 0.2$ – $0.3$  dex) is highly statistically significant.

#### 4.4. Star-formation Histories

Finally, we use the **Blast** tool from Jones et al. (2024)<sup>5</sup> to derive SED properties for the BB CCSN hosts, a

<sup>5</sup> <https://blast.scimma.org/>.

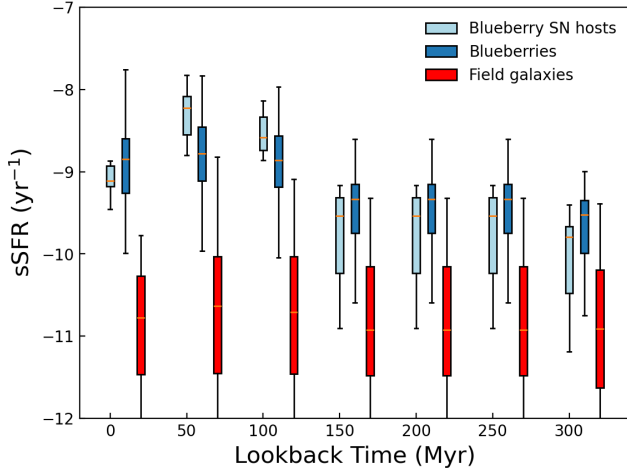


**Figure 9.** Box plot of the star formation history of SN hosts, BB galaxies, and SDSS field galaxies. The orange line represents the median SFR estimated by `Blast`, while the box edges represent 25 and 75 percentiles of the population, and the whiskers for  $\pm 1.5 \times$  the interquartile range, respectively. BB SN hosts show an elevated sSFR between  $\sim 30 - 100$  Myr, consistent with the CC SN delay time distribution (Zapartas et al. 2017; Castrillo et al. 2021; Saito et al. 2022). The SFH is computed from the `prospector- $\alpha$`  non-parametric model using bins of 0–30 Myr, 30–100 Myr, 100–300 Myr, and 300–1 Gyr.

randomly-selected subsample of BBs, and a randomly-selected subsample of field galaxies from SDSS (subsamples are necessary because computing SFHs for the full sample is computationally infeasible). `Blast` analyzes SN host properties by downloading archival images and automatically measuring matched-aperture photometry from archival SDSS (York et al. 2000), the Dark Energy Spectroscopic Instrument Legacy imaging Surveys (Dey et al. 2019), GALEX (Martin et al. 2005), WISE (Wright et al. 2010), Pan-STARRS (Chambers et al. 2016; Flewelling et al. 2020; Magnier et al. 2020), and 2MASS images (Skrutskie et al. 2006). It then uses the `Prospector- $\alpha$`  model (Leja et al. 2019; Johnson et al. 2021) to measure SED properties from this photometry, with a speed enhancement using simulation-based inference (Wang et al. 2023). With the `Prospector- $\alpha$`  model, `Blast` implements a non-parametric star-formation history across seven logarithmically spaced time bins.

Figure 9 plots the SFH of the SN hosts, BB galaxies, and SDSS field galaxies. BB galaxies show an overall elevated SFR compared to field galaxies. SN hosts specifically have a sSFR between lookback times of  $\sim 30 - 100$  Myr that is enhanced by 0.56 dex, and which is significant at the 99% confidence level (using a Mann-Whitney Test). This is consistent with expectations from the CC SN delay time distribution; the most mas-

sive SN progenitors (likely SN Ib or Ic) should explode in  $\sim 10$  Myr or less, while the least massive CC SN progenitors will be closer to 50 Myr between formation and explosion; this is consistent with the time frame of the observed starburst period. This spread in CC SN explosion timescales also allows time for changes in the ISM structure as a result of the injected mechanical energy, with  $\sim 2 - 3$  Myr typically needed for massive stars to clear out channels through the ISM via feedback winds and/or supernovae (Kimm et al. 2019; Naidu et al. 2022). However, the lower sSFR at the present time (as also seen in the lower panel of Figure 8), is consistent with our findings of lower O32 ratios and  $\xi_{\text{ion}}$  in SN host galaxies.

## 5. DISCUSSION AND CONCLUSIONS

In this study, we identified 11 SN events within 1242  $z < 0.12$  Blueberry (BB) galaxies. We find that SN host galaxies tend to exhibit elevated star formation rates, higher stellar masses, bursty star-formation histories, and have evidence for elevated UV escape fractions relative to non-host BBs. However, we also observe lower rates of ionizing photon production. Since GP and BB galaxies are widely regarded as analogs to early-universe Ly $\alpha$  emitters (LAEs), this gives us a unique tool for probing the role of SNe in facilitating ionizing photon escape during the EoR.

### 5.1. Implications for Reionization

Our analysis of UV slopes, a proxy for  $f_{\text{esc}}$ , finds modest evidence that BB galaxies that host SNe exhibit systematically steeper (more negative) UV slopes than the general BB population at  $2.1\sigma$  significance. Bluer UV continua are often considered tracers of young stellar populations and/or reduced dust attenuation, both of which lead to higher ionizing photon escape fractions. In Figure 7, we further demonstrate that several SN host galaxies lie in regions that are considered “cosmologically relevant” at  $f_{\text{esc}}^{\text{LyC}} > 5\%$ , implying they would meaningfully contribute to the ionizing photon budget of cosmic reionization, based on the relation from Chisholm et al. (2022). Taken together, the steeper UV slopes and their alignment with LyC escape regions provide indirect but compelling evidence that SNe may contribute meaningfully to the escape of ionizing radiation, and potentially play a key role in EoR feedback processes.

Furthermore, these findings may be aligned with feedback-driven reionization models (e.g., Jaskot & Oey 2014; Kimm et al. 2019; Flury et al. 2022a,b; Naidu et al. 2022; Flury et al. 2025), in which mechanical energy from SNe in stellar populations aged  $\sim 10 - 50$  Myr

clears dense ISM and circumgalactic medium (CGM) regions. Our star-formation histories of SN hosts suggest a typical peak of SFR within the last  $\sim$ 30–100 Myr, and ISM channels could form within 2–10 Myr of the first bursts of SNe (Naidu et al. 2022). Starburst episodes in compact SFGs may last long enough for young stars to produce ionizing radiation that escapes via these SN-created channels (Izotov et al. 2011; Jaskot & Oey 2014).

However, the number of ionizing photons that ultimately escape from a galaxy also depends on its intrinsic ionizing photon production efficiency,  $\xi_{\text{ion}}$ . We find that CC SN host galaxies exhibit lower  $\xi_{\text{ion}}$  compared to the non-host BB population with similar *FUV* absolute magnitudes, at 98% confidence. This implies that the intense burst of SFR that produced these SNe may begin to decrease on  $\sim$ 50 Myr timescales, whether due to SN-driven feedback or other processes, and suggests that establishing the timescale of substantial ionizing photon production is also an important factor in understanding whether the contribution of SNe to reionization is truly significant. Studies on high-resolution radiation-hydrodynamic simulations have pointed out high variation in escape fractions in dwarf galaxies, again emphasizing the importance in understanding the timescales of LyC escape and ionizing photon production in these systems (Trebitsch et al. 2017). While the first SNe should clear channels on timescales as short as 10 Myr, our results align with previous delay time measurements and show that the average CCSN originates from older progenitors.

These results also offer potential insight into the relative roles of more massive systems within models of cosmic reionization, particularly in the context of democratic versus oligarchic scenarios. The SN-host BB galaxies in our sample have higher stellar masses than the full BB sample, with  $\log(M_*/M_{\odot}) \sim 8.5 - 9.5$  and a peak around  $\sim 9.0$ , consistent with the dominant contributors to the oligarchic reionization scenario ( $\log(M_*/M_{\odot}) > 8.5$ , Naidu et al. 2020).

In democratic reionization models, galaxies at the brighter and more massive end are often assumed to contribute minimally to the ionizing photon budget because their higher halo masses suppress sustained escape, with elevated  $f_{\text{esc}}$  occurring only during brief, SN-driven episodes (Finkelstein et al. 2019). However, our findings suggest that SN-host galaxies, despite being more massive than the commonly invoked low-mass reionizers, can nonetheless exhibit signatures consistent with elevated escape fractions (e.g., steeper UV slopes). This implies that SN-driven feedback may facilitate non-

negligible ionizing photon escape even in deeper potential wells.

Although it is possible that SN feedback in more massive halos enables brief escape episodes, if CC SNe can be recurrent or clustered in highly SF galaxies, these episodes may also be repetitive and efficient (Mannucci et al. 2005; Anderson & Soto 2013). Unlike in low-mass halos, where SN feedback may suppress star formation, in more massive systems, feedback may promote intermittent transparency without fully quenching star formation, allowing for sustained or repeated episodes of LyC leaking. This may be especially relevant for compact SFGs undergoing multiple, possibly overlapping starburst phases, potentially similar to GP and BB galaxies. We also note that while SNe Ia are largely excluded from this analysis, they will also — despite their low correlation with ongoing SFR — inject additional, significant energy into the ISM of these galaxies, and should not be entirely neglected.

## 5.2. Future Work

This study is subject to several limitations. Most importantly, we are unable to directly observe the Ly $\alpha$  emission or LyC escape in these galaxies, as most only have optical spectra; we rely instead on indirect indicators such as UV slope and SFR estimates. We also note that recent studies show that some low-mass/faint galaxies in the early Universe ( $z \gtrsim 6$ ) can have limited star-formation efficiencies, and that these early UV-faint galaxies can have vastly diverse SFHs (Endsley et al. 2025). Therefore, whether local BBs are adequate analogs to the SFH of early galaxies is still a topic of debate.

Some of the observed trends, particularly the apparent suppression of SN rates in BB galaxies, may also be influenced by selection effects. For example, SNe occurring in very compact hosts can be systematically missed or misclassified; in particular, SNe in BB galaxies may be mistaken for AGN variability or otherwise blended with bright central emission. However, an intrinsic explanation cannot be ruled out: a reduced SN rate in compact galaxies could arise from differences in stellar populations, such as metallicity-driven mass function variations that suppress the formation of the most massive stars (Liang et al. 2024). Distinguishing between these possibilities will require more complete and in-depth transient searches. Given the current limitations, we regard the present rate measurements as provisional and highlight the need for more systematic SN searches in compact, low-mass star-forming galaxies.

Future FUV data from instruments like the Hubble Space Telescope’s (HST’s) Cosmic Origins Spectrograph

(COS) could more directly characterize Ly $\alpha$  emission and key ISM absorption diagnostics in these systems, including Si II (a neutral gas tracer), C II (cold gas), and C IV (hot gas and outflows). Additionally, Ly $\alpha$  profile analysis (e.g., peak separations, asymmetry, and equivalent widths) could be used to directly characterize the covering fraction and column density of neutral hydrogen (Yang et al. 2016; Izotov et al. 2016b). Multiple past HST/COS programs have observed a subset of GP galaxies, even including a known SN host (2021bk, included in this study), with focus on their Ly $\alpha$  profiles and UV emission lines (Duval et al. 2016; McPherson et al. 2023).

Increased sample sizes and higher-redshift SN observations of GP galaxies will soon be possible, particularly from the Vera C. Rubin Observatory’s Legacy Survey of Space and Time (LSST) and the *Roman Space Telescope*. Simultaneously, high-redshift galaxy observations with *JWST* will increase the sample of high- $z$  Ly $\alpha$  measurements during the EoR, providing crucial insights into the SN-driven feedback mechanisms shaping the earliest galaxies (Jaskot et al. 2024; Lin et al. 2024a; Ma et al. 2024; Dhandha et al. 2025; Willott et al. 2025), and other drivers of cosmic reionization.

## 6. ACKNOWLEDGEMENTS

## REFERENCES

Ahn, C. P., Alexandroff, R., Prieto, C. A., et al. 2014, The Astrophysical Journal Supplement Series, 211, 17, doi: [10.1088/0067-0049/211/2/17](https://doi.org/10.1088/0067-0049/211/2/17)

Albareti, F. D., Allende Prieto, C., Almeida, A., et al. 2017, The Astrophysical Journal Supplement Series, 233, 25, doi: [10.3847/1538-4365/aa8992](https://doi.org/10.3847/1538-4365/aa8992)

Amorín, R., Vilchez, J. M., Hägele, G. F., et al. 2012, The Astrophysical Journal, 754, L22, doi: [10.1088/2041-8205/754/2/L22](https://doi.org/10.1088/2041-8205/754/2/L22)

Anderson, J. P., & Soto, M. 2013, Astronomy and Astrophysics, 550, A69, doi: [10.1051/0004-6361/201220600](https://doi.org/10.1051/0004-6361/201220600)

Baldwin, J. A., Phillips, M. M., & Terlevich, R. 1981, Publications of the Astronomical Society of the Pacific, 93, 5, doi: [10.1086/130766](https://doi.org/10.1086/130766)

Barbary, K., Barclay, T., Biswas, R., et al. 2016, Astrophysics Source Code Library, ascl:1611.017. <https://ui.adsabs.harvard.edu/abs/2016ascl.soft11017B>

Barkana, R., & Loeb, A. 2001, Physics Reports, 349, 125, doi: [10.1016/S0370-1573\(01\)00019-9](https://doi.org/10.1016/S0370-1573(01)00019-9)

Becker, G. D., Bolton, J. S., Madau, P., et al. 2015, Monthly Notices of the Royal Astronomical Society, 447, 3402, doi: [10.1093/mnras/stu2646](https://doi.org/10.1093/mnras/stu2646)

Bellm, E. C., Kulkarni, S. R., Graham, M. J., et al. 2019, Publications of the Astronomical Society of the Pacific, 131, 018002, doi: [10.1088/1538-3873/aaecbe](https://doi.org/10.1088/1538-3873/aaecbe)

Berg, D. A., Skillman, E. D., Marble, A. R., et al. 2012, The Astrophysical Journal, 754, 98, doi: [10.1088/0004-637X/754/2/98](https://doi.org/10.1088/0004-637X/754/2/98)

Blain, A. W., Smail, I., Ivison, R. J., Kneib, J.-P., & Frayer, D. T. 2002, Physics Reports, 369, 111, doi: [10.1016/S0370-1573\(02\)00134-5](https://doi.org/10.1016/S0370-1573(02)00134-5)

Bouwens, R. J., Illingworth, G. D., Oesch, P. A., et al. 2014, The Astrophysical Journal, 793, 115, doi: [10.1088/0004-637X/793/2/115](https://doi.org/10.1088/0004-637X/793/2/115)

M.K. and D.O.J. acknowledge support from NSF grants AST-2407632, AST-2429450, and AST-2510993, NASA grant 80NSSC24M0023, and HST/JWST grants HST-GO-17128.028 and JWST-GO-05324.031, awarded by the Space Telescope Science Institute (STScI), which is operated by the Association of Universities for Research in Astronomy, Inc., for NASA, under contract NAS5-26555. N.E.D acknowledges support from NSF grants LEAPS-2532703 and AST-2510993.

Support for K.I. was provided by NASA through the NASA Hubble Fellowship grant HST-HF2-51508 awarded by the Space Telescope Science Institute, which is operated by the Association of Universities for Research in Astronomy, Inc., for NASA, under contract NAS5-26555.

B.C.L. is supported by the international Gemini Observatory, a program of NSF NOIRLab, which is managed by the Association of Universities for Research in Astronomy (AURA) under a cooperative agreement with the U.S. National Science Foundation, on behalf of the Gemini partnership of Argentina, Brazil, Canada, Chile, the Republic of Korea, and the United States of America.

W.B.H. acknowledges support from the National Science Foundation Graduate Research Fellowship Program under Grant No. 2236415.

The authors wish to recognize and acknowledge the cultural role and reverence that the summit of Maunakea has always had within the indigenous Hawaiian community.

Brough, S., Collins, C., DeMarco, R., et al. 2020, The Vera Rubin Observatory Legacy Survey of Space and Time and the Low Surface Brightness Universe, arXiv, doi: [10.48550/arXiv.2001.11067](https://doi.org/10.48550/arXiv.2001.11067)

Bussmann, R. S., Riechers, D., Fialkov, A., et al. 2015, The Astrophysical Journal, 812, 43, doi: [10.1088/0004-637X/812/1/43](https://doi.org/10.1088/0004-637X/812/1/43)

Calzetti, D., Kinney, A. L., & Storchi-Bergmann, T. 1994, The Astrophysical Journal, 429, 582, doi: [10.1086/174346](https://doi.org/10.1086/174346)

Cardamone, C. N., Schawinski, K., Sarzi, M., et al. 2009, Monthly Notices of the Royal Astronomical Society, 399, 1191, doi: [10.1111/j.1365-2966.2009.15383.x](https://doi.org/10.1111/j.1365-2966.2009.15383.x)

Casey, C. M., Narayanan, D., & Cooray, A. 2014, Physics Reports, 541, 45, doi: [10.1016/j.physrep.2014.02.009](https://doi.org/10.1016/j.physrep.2014.02.009)

Castrillo, A., Ascasibar, Y., Galbany, L., et al. 2021, Monthly Notices of the Royal Astronomical Society, 501, 3122, doi: [10.1093/mnras/staa3876](https://doi.org/10.1093/mnras/staa3876)

Chabrier, G. 2003, Publications of the Astronomical Society of the Pacific, 115, 763, doi: [10.1086/376392](https://doi.org/10.1086/376392)

Chambers, K. C., Magnier, E. A., Metcalfe, N., et al. 2016, The Pan-STARRS1 Surveys, doi: [10.48550/arXiv.1612.05560](https://doi.org/10.48550/arXiv.1612.05560)

Chapman, S. C., Blain, A. W., Smail, I., & Ivison, R. J. 2005, The Astrophysical Journal, 622, 772, doi: [10.1086/428082](https://doi.org/10.1086/428082)

Chen, Y.-M., Kauffmann, G., Tremonti, C. A., et al. 2012, Monthly Notices of the Royal Astronomical Society, 421, 314, doi: [10.1111/j.1365-2966.2011.20306.x](https://doi.org/10.1111/j.1365-2966.2011.20306.x)

Chisholm, J., Saldana-Lopez, A., Flury, S., et al. 2022, Monthly Notices of the Royal Astronomical Society, 517, 5104, doi: [10.1093/mnras/stac2874](https://doi.org/10.1093/mnras/stac2874)

Clarke, C., & Oey, M. S. 2002, Monthly Notices of the Royal Astronomical Society, 337, 1299, doi: [10.1046/j.1365-8711.2002.05976.x](https://doi.org/10.1046/j.1365-8711.2002.05976.x)

Cordier, B., Wei, J. Y., Tanvir, N. R., et al. 2025, Astronomy and Astrophysics, 704, L7, doi: [10.1051/0004-6361/202556580](https://doi.org/10.1051/0004-6361/202556580)

Coulter, D. A., Pierel, J. D. R., DeCoursey, C., et al. 2025, Discovery of a likely Type II SN at  $z=3.6$  with JWST, arXiv, doi: [10.48550/arXiv.2501.05513](https://doi.org/10.48550/arXiv.2501.05513)

Dayal, P., & Ferrara, A. 2018, Physics Reports, 780, 1, doi: [10.1016/j.physrep.2018.10.002](https://doi.org/10.1016/j.physrep.2018.10.002)

Dayal, P., Volonteri, M., Choudhury, T. R., et al. 2020, Monthly Notices of the Royal Astronomical Society, 495, 3065, doi: [10.1093/mnras/staa1138](https://doi.org/10.1093/mnras/staa1138)

DeCoursey, C., Egami, E., Pierel, J. D. R., et al. 2024, The JADES Transient Survey: Discovery and Classification of Supernovae in the JADES Deep Field, arXiv, <http://arxiv.org/abs/2406.05060>

DeCoursey, C., Egami, E., Sun, F., et al. 2025, The First Photometric Evidence of a Transient/Variable Source at  $z>5$  with JWST, arXiv, doi: [10.48550/arXiv.2504.17007](https://doi.org/10.48550/arXiv.2504.17007)

Desai, D. D., Kochanek, C. S., Shappee, B. J., et al. 2024, Monthly Notices of the Royal Astronomical Society, 530, 5016, doi: [10.1093/mnras/stae606](https://doi.org/10.1093/mnras/stae606)

Dey, A., Schlegel, D. J., Lang, D., et al. 2019, The Astronomical Journal, 157, 168, doi: [10.3847/1538-3881/ab089d](https://doi.org/10.3847/1538-3881/ab089d)

Dhandha, J., Fialkov, A., Gessey-Jones, T., et al. 2025, Monthly Notices of the Royal Astronomical Society, 542, 2292, doi: [10.1093/mnras/staf1359](https://doi.org/10.1093/mnras/staf1359)

Dilday, B., Kessler, R., Frieman, J. A., et al. 2008, The Astrophysical Journal, 682, 262, doi: [10.1086/587733](https://doi.org/10.1086/587733)

Duval, F., Östlin, G., Hayes, M., et al. 2016, Astronomy & Astrophysics, 587, A77, doi: [10.1051/0004-6361/201526876](https://doi.org/10.1051/0004-6361/201526876)

Emami, N., Siana, B., Alavi, A., et al. 2020, The Astrophysical Journal, 895, 116, doi: [10.3847/1538-4357/ab8f97](https://doi.org/10.3847/1538-4357/ab8f97)

Endsley, R., Chisholm, J., Stark, D. P., Topping, M. W., & Whitler, L. 2025, The Astrophysical Journal, 987, 189, doi: [10.3847/1538-4357/addc74](https://doi.org/10.3847/1538-4357/addc74)

Fan, X., Carilli, C. L., & Keating, B. 2006a, Annual Review of Astronomy and Astrophysics, 44, 415, doi: [10.1146/annurev.astro.44.051905.092514](https://doi.org/10.1146/annurev.astro.44.051905.092514)

Fan, X., Strauss, M. A., Becker, R. H., et al. 2006b, The Astronomical Journal, 132, 117, doi: [10.1086/504836](https://doi.org/10.1086/504836)

Fernandez, E. R., & Shull, J. M. 2011, The Astrophysical Journal, 731, 20, doi: [10.1088/0004-637X/731/1/20](https://doi.org/10.1088/0004-637X/731/1/20)

Finkelstein, S. L., Ryan, Jr., R. E., Papovich, C., et al. 2015, The Astrophysical Journal, 810, 71, doi: [10.1088/0004-637X/810/1/71](https://doi.org/10.1088/0004-637X/810/1/71)

Finkelstein, S. L., D'Aloisio, A., Paardekooper, J.-P., et al. 2019, The Astrophysical Journal, 879, 36, doi: [10.3847/1538-4357/ab1ea8](https://doi.org/10.3847/1538-4357/ab1ea8)

Flewelling, H. A., Magnier, E. A., Chambers, K. C., et al. 2020, The Astrophysical Journal Supplement Series, 251, 7, doi: [10.3847/1538-4365/abb82d](https://doi.org/10.3847/1538-4365/abb82d)

Flores Velázquez, J. A., Gurvich, A. B., Faucher-Giguère, C.-A., et al. 2021, Monthly Notices of the Royal Astronomical Society, 501, 4812, doi: [10.1093/mnras/staa3893](https://doi.org/10.1093/mnras/staa3893)

Flury, S. R., Jaskot, A. E., Ferguson, H. C., et al. 2022a, The Astrophysical Journal Supplement Series, 260, 1, doi: [10.3847/1538-4365/ac5331](https://doi.org/10.3847/1538-4365/ac5331)

—. 2022b, The Astrophysical Journal, 930, 126, doi: [10.3847/1538-4357/ac61e4](https://doi.org/10.3847/1538-4357/ac61e4)

Flury, S. R., Jaskot, A. E., Saldana-Lopez, A., et al. 2025, *The Astrophysical Journal*, 985, 128, doi: [10.3847/1538-4357/adc305](https://doi.org/10.3847/1538-4357/adc305)

Furlanetto, S. R., Oh, S. P., & Briggs, F. H. 2006, *Physics Reports*, 433, 181, doi: [10.1016/j.physrep.2006.08.002](https://doi.org/10.1016/j.physrep.2006.08.002)

Furlanetto, S. R., Zaldarriaga, M., & Hernquist, L. 2004, *The Astrophysical Journal*, 613, 1, doi: [10.1086/423025](https://doi.org/10.1086/423025)

Gagliano, A., Narayan, G., Engel, A., Carrasco Kind, M., & Collaboration, L. D. E. S. 2021, *The Astrophysical Journal*, 908, 170, doi: [10.3847/1538-4357/abd02b](https://doi.org/10.3847/1538-4357/abd02b)

Gnedin, N. Y., Kravtsov, A. V., & Chen, H.-W. 2008, *The Astrophysical Journal*, 672, 765, doi: [10.1086/524007](https://doi.org/10.1086/524007)

Heckman, T. M., Sembach, K. R., Meurer, G. R., et al. 2001, *The Astrophysical Journal*, 558, 56, doi: [10.1086/322475](https://doi.org/10.1086/322475)

Heckman, T. M., Borthakur, S., Overzier, R., et al. 2011, *The Astrophysical Journal*, 730, 5, doi: [10.1088/0004-637X/730/1/5](https://doi.org/10.1088/0004-637X/730/1/5)

Hinshaw, G., Larson, D., Komatsu, E., et al. 2013, *The Astrophysical Journal Supplement Series*, 208, 19, doi: [10.1088/0067-0049/208/2/19](https://doi.org/10.1088/0067-0049/208/2/19)

Hoogendam, W. B., Shappee, B. J., Brown, P. J., et al. 2024, *The Astrophysical Journal*, 966, 139, doi: [10.3847/1538-4357/ad33ba](https://doi.org/10.3847/1538-4357/ad33ba)

Huber, M., Chambers, K. C., Flewelling, H., et al. 2015, *The Astronomer's Telegram*, 7153, 1, <https://ui.adsabs.harvard.edu/abs/2015ATel.7153....1H>

Izotov, Y. I., Guseva, N. G., Fricke, K. J., & Henkel, C. 2015, *Monthly Notices of the Royal Astronomical Society*, 451, 2251, doi: [10.1093/mnras/stv1115](https://doi.org/10.1093/mnras/stv1115)

Izotov, Y. I., Guseva, N. G., Fricke, K. J., et al. 2021, *Astronomy and Astrophysics*, 646, A138, doi: [10.1051/0004-6361/202039772](https://doi.org/10.1051/0004-6361/202039772)

Izotov, Y. I., Guseva, N. G., & Thuan, T. X. 2011, *The Astrophysical Journal*, 728, 161, doi: [10.1088/0004-637X/728/2/161](https://doi.org/10.1088/0004-637X/728/2/161)

Izotov, Y. I., Orlitová, I., Schaerer, D., et al. 2016a, *Nature*, 529, 178, doi: [10.1038/nature16456](https://doi.org/10.1038/nature16456)

Izotov, Y. I., Schaerer, D., Thuan, T. X., et al. 2016b, *Monthly Notices of the Royal Astronomical Society*, 461, 3683, doi: [10.1093/mnras/stw1205](https://doi.org/10.1093/mnras/stw1205)

Jaskot, A. E., & Oey, M. S. 2014, *The Origin and Optical Depth of Ionizing Photons in the Green Pea Galaxies*, eprint: arXiv:1402.4429: arXiv, doi: [10.48550/arXiv.1402.4429](https://doi.org/10.48550/arXiv.1402.4429)

Jaskot, A. E., Silveyra, A. C., Plantinga, A., et al. 2024, *The Astrophysical Journal*, 973, 111, doi: [10.3847/1538-4357/ad5557](https://doi.org/10.3847/1538-4357/ad5557)

Jiang, D., Jiang, L., Sun, S., Liu, W., & Fu, S. 2025, *Nature Astronomy*, 9, 1890, doi: [10.1038/s41550-025-02676-7](https://doi.org/10.1038/s41550-025-02676-7)

Jiang, T., Malhotra, S., Rhoads, J. E., & Yang, H. 2019, *The Astrophysical Journal*, 872, 145, doi: [10.3847/1538-4357/aaee8a](https://doi.org/10.3847/1538-4357/aaee8a)

Johnson, B. D., Leja, J., Conroy, C., & Speagle, J. S. 2021, *The Astrophysical Journal Supplement Series*, 254, 22, doi: [10.3847/1538-4365/abef67](https://doi.org/10.3847/1538-4365/abef67)

Jones, D. O., McGill, P., Manning, T. A., et al. 2024, *Blast: a Web Application for Characterizing the Host Galaxies of Astrophysical Transients*, doi: [10.48550/arXiv.2410.17322](https://doi.org/10.48550/arXiv.2410.17322)

Keller, B. W., & Kruijssen, J. M. D. 2022, *Monthly Notices of the Royal Astronomical Society*, 512, 199, doi: [10.1093/mnras/stac511](https://doi.org/10.1093/mnras/stac511)

Kennicutt, R. C., & Evans, N. J. 2012, *Annual Review of Astronomy and Astrophysics*, 50, 531, doi: [10.1146/annurev-astro-081811-125610](https://doi.org/10.1146/annurev-astro-081811-125610)

Kennicutt, Jr., R. C., Tamblyn, P., & Congdon, C. E. 1994, *The Astrophysical Journal*, 435, 22, doi: [10.1086/174790](https://doi.org/10.1086/174790)

Kenworthy, W. D., Jones, D. O., Dai, M., et al. 2021, *The Astrophysical Journal*, 923, 265, doi: [10.3847/1538-4357/ac30d8](https://doi.org/10.3847/1538-4357/ac30d8)

Kim, K. J., Malhotra, S., Rhoads, J. E., & Yang, H. 2021, *The Astrophysical Journal*, 914, 2, doi: [10.3847/1538-4357/abf833](https://doi.org/10.3847/1538-4357/abf833)

Kimm, T., Blaizot, J., Garel, T., et al. 2019, *Monthly Notices of the Royal Astronomical Society*, 486, 2215, doi: [10.1093/mnras/stz989](https://doi.org/10.1093/mnras/stz989)

Kimm, T., & Cen, R. 2014, *The Astrophysical Journal*, 788, 121, doi: [10.1088/0004-637X/788/2/121](https://doi.org/10.1088/0004-637X/788/2/121)

Leja, J., Carnall, A. C., Johnson, B. D., Conroy, C., & Speagle, J. S. 2019, *The Astrophysical Journal*, 876, 3, doi: [10.3847/1538-4357/ab133c](https://doi.org/10.3847/1538-4357/ab133c)

Levan, A. J., Schneider, B., Le Floc'h, E., et al. 2025, *Astronomy and Astrophysics*, 704, L8, doi: [10.1051/0004-6361/202556581](https://doi.org/10.1051/0004-6361/202556581)

Levi, M., Allen, L. E., Raichoor, A., et al. 2019, *The Dark Energy Spectroscopic Instrument (DESI)*, eprint: arXiv:1907.10688: arXiv, doi: [10.48550/arXiv.1907.10688](https://doi.org/10.48550/arXiv.1907.10688)

Lewis, J. S. W., Ocvirk, P., Dubois, Y., et al. 2023, *Monthly Notices of the Royal Astronomical Society*, 519, 5987, doi: [10.1093/mnras/stad081](https://doi.org/10.1093/mnras/stad081)

Li, W., Chornock, R., Leaman, J., et al. 2011, *Monthly Notices of the Royal Astronomical Society*, 412, 1473, doi: [10.1111/j.1365-2966.2011.18162.x](https://doi.org/10.1111/j.1365-2966.2011.18162.x)

Liang, Z., Suzuki, N., Doi, M., Tanaka, M., & Yasuda, N. 2024, *The Astrophysical Journal*, 970, 52, doi: [10.3847/1538-4357/ad4b19](https://doi.org/10.3847/1538-4357/ad4b19)

Lin, R., Zheng, Z.-Y., Jiang, C., et al. 2025, *The Astrophysical Journal Letters*, 980, L34, doi: [10.3847/2041-8213/adaaf1](https://doi.org/10.3847/2041-8213/adaaf1)

Lin, X., Cai, Z., Wu, Y., et al. 2024a, The Astrophysical Journal Supplement Series, 272, 33, doi: [10.3847/1538-4365/ad3e7d](https://doi.org/10.3847/1538-4365/ad3e7d)

Lin, Y.-H., Scarlata, C., Williams, H., et al. 2024b, Monthly Notices of the Royal Astronomical Society, 527, 4173, doi: [10.1093/mnras/stad3483](https://doi.org/10.1093/mnras/stad3483)

Liu, S., Luo, A. L., Yang, H., et al. 2022, The Astrophysical Journal, 927, 57, doi: [10.3847/1538-4357/ac4bd9](https://doi.org/10.3847/1538-4357/ac4bd9)

Llerena, M., Amorín, R., Pentericci, L., et al. 2023, Astronomy and Astrophysics, 676, A53, doi: [10.1051/0004-6361/202346232](https://doi.org/10.1051/0004-6361/202346232)

Luo, A. L., Zhang, Y.-X., & Zhao, Y.-H. 2004, Advanced Software, Control, and Communication Systems for Astronomy, 5496, 756, doi: [10.1117/12.548737](https://doi.org/10.1117/12.548737)

Ma, X., Hopkins, P. F., Kasen, D., et al. 2016, Monthly Notices of the Royal Astronomical Society, 459, 3614, doi: [10.1093/mnras/stw941](https://doi.org/10.1093/mnras/stw941)

Ma, X., Quataert, E., Wetzel, A., et al. 2020, Monthly Notices of the Royal Astronomical Society, 498, 2001, doi: [10.1093/mnras/staa2404](https://doi.org/10.1093/mnras/staa2404)

Ma, Z., Sun, B., Cheng, C., et al. 2024, The Astrophysical Journal, 975, 87, doi: [10.3847/1538-4357/ad7b32](https://doi.org/10.3847/1538-4357/ad7b32)

Madau, P., & Dickinson, M. 2014, Annual Review of Astronomy and Astrophysics, 52, 415, doi: [10.1146/annurev-astro-081811-125615](https://doi.org/10.1146/annurev-astro-081811-125615)

Madau, P., Giallongo, E., Grazian, A., & Haardt, F. 2024, Cosmic Reionization in the JWST Era: Back to AGNs?, arXiv, doi: [10.48550/arXiv.2406.18697](https://doi.org/10.48550/arXiv.2406.18697)

Madau, P., & Haardt, F. 2015, The Astrophysical Journal, 813, L8, doi: [10.1088/2041-8205/813/1/L8](https://doi.org/10.1088/2041-8205/813/1/L8)

Madau, P., Haardt, F., & Rees, M. J. 1999, The Astrophysical Journal, 514, 648, doi: [10.1086/306975](https://doi.org/10.1086/306975)

Magnier, E. A., Schlafly, E. F., Finkbeiner, D. P., et al. 2020, The Astrophysical Journal Supplement Series, 251, 6, doi: [10.3847/1538-4365/abb82a](https://doi.org/10.3847/1538-4365/abb82a)

Mannucci, F., Della Valle, M., Panagia, N., et al. 2005, Astronomy and Astrophysics, 433, 807, doi: [10.1051/0004-6361:20041411](https://doi.org/10.1051/0004-6361:20041411)

Maoz, D., Mannucci, F., & Nelemans, G. 2014, Annual Review of Astronomy and Astrophysics, 52, 107, doi: [10.1146/annurev-astro-082812-141031](https://doi.org/10.1146/annurev-astro-082812-141031)

Maraston, C., Pforr, J., Henriques, B. M., et al. 2013, Monthly Notices of the Royal Astronomical Society, 435, 2764, doi: [10.1093/mnras/stt1424](https://doi.org/10.1093/mnras/stt1424)

Martin, D. C., Fanson, J., Schiminovich, D., et al. 2005, The Astrophysical Journal, 619, L1, doi: [10.1086/426387](https://doi.org/10.1086/426387)

Masci, F. J., Laher, R. R., Rusholme, B., et al. 2019, Publications of the Astronomical Society of the Pacific, 131, 018003, doi: [10.1088/1538-3873/aae8ac](https://doi.org/10.1088/1538-3873/aae8ac)

Mascia, S., Pentericci, L., Calabrò, A., et al. 2024, Astronomy and Astrophysics, 685, A3, doi: [10.1051/0004-6361/202347884](https://doi.org/10.1051/0004-6361/202347884)

Matthee, J., Naidu, R. P., Pezzulli, G., et al. 2022, Monthly Notices of the Royal Astronomical Society, 512, 5960, doi: [10.1093/mnras/stac801](https://doi.org/10.1093/mnras/stac801)

McGreer, I. D., Mesinger, A., & D'Odorico, V. 2015, Monthly Notices of the Royal Astronomical Society, 447, 499, doi: [10.1093/mnras/stu2449](https://doi.org/10.1093/mnras/stu2449)

McPherson, D. K., Fisher, D. B., Nielsen, N. M., et al. 2023, Monthly Notices of the Royal Astronomical Society, 525, 6170, doi: [10.1093/mnras/stad2685](https://doi.org/10.1093/mnras/stad2685)

Naidu, R. P., Tacchella, S., Mason, C. A., et al. 2020, The Astrophysical Journal, 892, 109, doi: [10.3847/1538-4357/ab7cc9](https://doi.org/10.3847/1538-4357/ab7cc9)

Naidu, R. P., Matthee, J., Oesch, P. A., et al. 2022, Monthly Notices of the Royal Astronomical Society, 510, 4582, doi: [10.1093/mnras/stab3601](https://doi.org/10.1093/mnras/stab3601)

Nakajima, K., & Ouchi, M. 2014, Monthly Notices of the Royal Astronomical Society, 442, 900, doi: [10.1093/mnras/stu902](https://doi.org/10.1093/mnras/stu902)

Nelson, D., Pillepich, A., Springel, V., et al. 2019, Monthly Notices of the Royal Astronomical Society, 490, 3234, doi: [10.1093/mnras/stz2306](https://doi.org/10.1093/mnras/stz2306)

Nugent, A. E., Villar, V. A., Gagliano, A., et al. 2026, The Astrophysical Journal, 997, 38, doi: [10.3847/1538-4357/ae247b](https://doi.org/10.3847/1538-4357/ae247b)

Observations Time Allocation Committee, R., & Community Survey Definition Committees, C. 2025, Roman Observations Time Allocation Committee: Final Report and Recommendations, arXiv, doi: [10.48550/arXiv.2505.10574](https://doi.org/10.48550/arXiv.2505.10574)

Paardekooper, J. P., Khochfar, S., & Dalla, C. V. 2013, Monthly Notices of the Royal Astronomical Society, 429, L94, doi: [10.1093/mnrasl/sls032](https://doi.org/10.1093/mnrasl/sls032)

Paardekooper, J.-P., Khochfar, S., & Dalla Vecchia, C. 2015, Monthly Notices of the Royal Astronomical Society, 451, 2544, doi: [10.1093/mnras/stv1114](https://doi.org/10.1093/mnras/stv1114)

Pierel, J. D. R., Jones, D. O., Kenworthy, W. D., et al. 2022, The Astrophysical Journal, 939, 11, doi: [10.3847/1538-4357/ac93f9](https://doi.org/10.3847/1538-4357/ac93f9)

Planck Collaboration, Aghanim, N., Akrami, Y., et al. 2020, Astronomy and Astrophysics, 641, A6, doi: [10.1051/0004-6361/201833910](https://doi.org/10.1051/0004-6361/201833910)

Raiter, A., Schaerer, D., & Fosbury, R. A. E. 2010, Astronomy and Astrophysics, 523, A64, doi: [10.1051/0004-6361/201015236](https://doi.org/10.1051/0004-6361/201015236)

Razoumov, A. O., & Sommer-Larsen, J. 2010, The Astrophysical Journal, 710, 1239, doi: [10.1088/0004-637X/710/2/1239](https://doi.org/10.1088/0004-637X/710/2/1239)

Reddy, N. A., Kriek, M., Shapley, A. E., et al. 2015, *The Astrophysical Journal*, 806, 259, doi: [10.1088/0004-637X/806/2/259](https://doi.org/10.1088/0004-637X/806/2/259)

Richards, G. T., Strauss, M. A., Fan, X., et al. 2006, *The Astronomical Journal*, 131, 2766, doi: [10.1086/503559](https://doi.org/10.1086/503559)

Rigault, M., Aldering, G., Kowalski, M., et al. 2015, *The Astrophysical Journal*, 802, 20, doi: [10.1088/0004-637X/802/1/20](https://doi.org/10.1088/0004-637X/802/1/20)

Rinaldi, P., Caputi, K. I., Iani, E., et al. 2024, *The Astrophysical Journal*, 969, 12, doi: [10.3847/1538-4357/ad4147](https://doi.org/10.3847/1538-4357/ad4147)

Robertson, B. E. 2022, *Annual Review of Astronomy and Astrophysics*, 60, 121, doi: [10.1146/annurev-astro-120221-044656](https://doi.org/10.1146/annurev-astro-120221-044656)

Robertson, B. E., Ellis, R. S., Furlanetto, S. R., & Dunlop, J. S. 2015, *The Astrophysical Journal*, 802, L19, doi: [10.1088/2041-8205/802/2/L19](https://doi.org/10.1088/2041-8205/802/2/L19)

Rodney, S. A., Riess, A. G., Strolger, L.-G., et al. 2014, *The Astronomical Journal*, 148, 13, doi: [10.1088/0004-6256/148/1/13](https://doi.org/10.1088/0004-6256/148/1/13)

Roediger, J. C., & Courteau, S. 2015, *Monthly Notices of the Royal Astronomical Society*, 452, 3209, doi: [10.1093/mnras/stv1499](https://doi.org/10.1093/mnras/stv1499)

Rogers, A. B., McLure, R. J., & Dunlop, J. S. 2013, *Monthly Notices of the Royal Astronomical Society*, 429, 2456, doi: [10.1093/mnras/sts515](https://doi.org/10.1093/mnras/sts515)

Rose, B. M., Baltay, C., Hounsell, R., et al. 2021, A Reference Survey for Supernova Cosmology with the Nancy Grace Roman Space Telescope, arXiv, doi: [10.48550/arXiv.2111.03081](https://doi.org/10.48550/arXiv.2111.03081)

Rose, B. M., Vincenzi, M., Hounsell, R., et al. 2025, *The Astrophysical Journal*, 988, 65, doi: [10.3847/1538-4357/ade1d6](https://doi.org/10.3847/1538-4357/ade1d6)

Saito, S., Tanaka, M., Sawada, R., & Moriya, T. J. 2022, *The Astrophysical Journal*, 931, 153, doi: [10.3847/1538-4357/ac6bec](https://doi.org/10.3847/1538-4357/ac6bec)

Saldana-Lopez, A., Schaerer, D., Chisholm, J., et al. 2022, *Astronomy and Astrophysics*, 663, A59, doi: [10.1051/0004-6361/202141864](https://doi.org/10.1051/0004-6361/202141864)

Salim, S., Rich, R. M., Charlot, S., et al. 2007, *The Astrophysical Journal Supplement Series*, 173, 267, doi: [10.1086/519218](https://doi.org/10.1086/519218)

Sanders, N. E., Soderberg, A. M., Valenti, S., et al. 2012, *The Astrophysical Journal*, 756, 184, doi: [10.1088/0004-637X/756/2/184](https://doi.org/10.1088/0004-637X/756/2/184)

Schaerer, D., Marques-Chaves, R., Barrufet, L., et al. 2022, *Astronomy and Astrophysics*, 665, L4, doi: [10.1051/0004-6361/202244556](https://doi.org/10.1051/0004-6361/202244556)

Schlafly, E. F., & Finkbeiner, D. P. 2011, *The Astrophysical Journal*, 737, 103, doi: [10.1088/0004-637X/737/2/103](https://doi.org/10.1088/0004-637X/737/2/103)

Schlegel, D. J., Finkbeiner, D. P., & Davis, M. 1998, *The Astrophysical Journal*, 500, 525, doi: [10.1086/305772](https://doi.org/10.1086/305772)

Schroeder, J., Mesinger, A., & Haiman, Z. 2013, *Monthly Notices of the Royal Astronomical Society*, 428, 3058, doi: [10.1093/mnras/sts253](https://doi.org/10.1093/mnras/sts253)

Senchyna, P., Stark, D. P., Vidal-García, A., et al. 2017, *Monthly Notices of the Royal Astronomical Society*, 472, 2608, doi: [10.1093/mnras/stx2059](https://doi.org/10.1093/mnras/stx2059)

Shah, E. A., Lemaux, B. C., Forrest, B., et al. 2024, Enhanced AGN Activity in Overdense Galactic Environments at  $2 < z < 4$ , arXiv, doi: [10.48550/arXiv.2409.02996](https://doi.org/10.48550/arXiv.2409.02996)

Shapley, A. E., Steidel, C. C., Pettini, M., Adelberger, K. L., & Erb, D. K. 2006, *The Astrophysical Journal*, 651, 688, doi: [10.1086/507511](https://doi.org/10.1086/507511)

Shappee, B., Prieto, J., Stanek, K. Z., et al. 2014, *American Astronomical Society*, 223, 236.03, <https://ui.adsabs.harvard.edu/abs/2014AAS...22323603S>

Sharma, M., Theuns, T., Frenk, C., et al. 2016, *Monthly Notices of the Royal Astronomical Society*, 458, L94, doi: [10.1093/mnrasl/slw021](https://doi.org/10.1093/mnrasl/slw021)

Shingles, L., Smith, K. W., Young, D. R., et al. 2021, Transient Name Server AstroNote, 7, 1, <https://ui.adsabs.harvard.edu/abs/2021TNSAN...7....1S>

Skrutskie, M. F., Cutri, R. M., Stiening, R., et al. 2006, *The Astronomical Journal*, 131, 1163, doi: [10.1086/498708](https://doi.org/10.1086/498708)

Smith, K. W., Smartt, S. J., Young, D. R., et al. 2020, *Publications of the Astronomical Society of the Pacific*, 132, 085002, doi: [10.1088/1538-3873/ab936e](https://doi.org/10.1088/1538-3873/ab936e)

Sorba, R., & Sawicki, M. 2015, *Monthly Notices of the Royal Astronomical Society*, 452, 235, doi: [10.1093/mnras/stv1235](https://doi.org/10.1093/mnras/stv1235)

Stoughton, C., Lupton, R. H., Bernardi, M., et al. 2002, *The Astronomical Journal*, 123, 485, doi: [10.1086/324741](https://doi.org/10.1086/324741)

Strolger, L.-G., Dahmen, T., Rodney, S. A., et al. 2015, *The Astrophysical Journal*, 813, 93, doi: [10.1088/0004-637X/813/2/93](https://doi.org/10.1088/0004-637X/813/2/93)

Taylor, E. N., Hopkins, A. M., Baldry, I. K., et al. 2011, *Monthly Notices of the Royal Astronomical Society*, 418, 1587, doi: [10.1111/j.1365-2966.2011.19536.x](https://doi.org/10.1111/j.1365-2966.2011.19536.x)

Thomas, D., Steele, O., Maraston, C., et al. 2013, *Monthly Notices of the Royal Astronomical Society*, 431, 1383, doi: [10.1093/mnras/stt261](https://doi.org/10.1093/mnras/stt261)

Tilvi, V., Malhotra, S., Rhoads, J. E., et al. 2020, *The Astrophysical Journal Letters*, 891, L10, doi: [10.3847/2041-8213/ab75ec](https://doi.org/10.3847/2041-8213/ab75ec)

Tonry, J. L., Denneau, L., Heinze, A. N., et al. 2018, *Publications of the Astronomical Society of the Pacific*, 130, 064505, doi: [10.1088/1538-3873/aabadf](https://doi.org/10.1088/1538-3873/aabadf)

Trebitsch, M., Blaizot, J., Rosdahl, J., Devriendt, J., & Slyz, A. 2017, Monthly Notices of the Royal Astronomical Society, 470, 224, doi: [10.1093/mnras/stx1060](https://doi.org/10.1093/mnras/stx1060)

Wang, B., Leja, J., Villar, V. A., & Speagle, J. S. 2023, The Astrophysical Journal Letters, 952, L10, doi: [10.3847/2041-8213/ace361](https://doi.org/10.3847/2041-8213/ace361)

Willott, C. J., Asada, Y., Iyer, K. G., et al. 2025, The Astrophysical Journal, 988, 26, doi: [10.3847/1538-4357/addir49](https://doi.org/10.3847/1538-4357/addir49)

Wise, J. H., & Cen, R. 2009, The Astrophysical Journal, 693, 984, doi: [10.1088/0004-637X/693/1/984](https://doi.org/10.1088/0004-637X/693/1/984)

Wise, J. H., Demchenko, V. G., Halicek, M. T., et al. 2014, Monthly Notices of the Royal Astronomical Society, 442, 2560, doi: [10.1093/mnras/stu979](https://doi.org/10.1093/mnras/stu979)

Wright, E. L., Eisenhardt, P. R. M., Mainzer, A. K., et al. 2010, The Astronomical Journal, 140, 1868, doi: [10.1088/0004-6256/140/6/1868](https://doi.org/10.1088/0004-6256/140/6/1868)

Yang, H., Malhotra, S., Gronke, M., et al. 2016, The Astrophysical Journal, 820, 130, doi: [10.3847/0004-637X/820/2/130](https://doi.org/10.3847/0004-637X/820/2/130)

Yang, H., Malhotra, S., Rhoads, J. E., et al. 2017, The Astrophysical Journal, 838, 4, doi: [10.3847/1538-4357/aa6337](https://doi.org/10.3847/1538-4357/aa6337)

York, D. G., Adelman, J., Anderson, Jr., J. E., et al. 2000, The Astronomical Journal, 120, 1579, doi: [10.1086/301513](https://doi.org/10.1086/301513)

Zackrisson, E., Inoue, A. K., & Jensen, H. 2013, The Astrophysical Journal, 777, 39, doi: [10.1088/0004-637X/777/1/39](https://doi.org/10.1088/0004-637X/777/1/39)

Zapartas, E., de Mink, S. E., Izzard, R. G., et al. 2017, Astronomy and Astrophysics, 601, A29, doi: [10.1051/0004-6361/201629685](https://doi.org/10.1051/0004-6361/201629685)

Zaroubi, S. 2013, in The First Galaxies, Vol. 396 (eprint: arXiv:1206.0267: Springer-Verlag Berlin Heidelberg), 45, doi: [10.1007/978-3-642-32362-1\\_2](https://doi.org/10.1007/978-3-642-32362-1_2)